Available online at www.sciencedirect.com
ScienceDirect
Geochimica et Cosmochimica Acta 70 (2006) 4643–4662
Geochimica
www.elsevier.com/locate/gca

Molybdenum and uranium geochemistry in continental margin sediments: Paleoproxy potential

James McManus [a,*], William M. Berelson [b], Silke Severmann [c], Rebecca L. Poulson [a], Douglas E. Hammond [b], Gary P. Klinkhammer [a], Chris Holm [a]

[a] Oregon State University, College of Oceanic and Atmospheric Sciences, 104 Ocean Admin. Bldg., Corvallis, OR 97331-5503, USA
[b] University of Southern California, Department of Earth Sciences, Los Angeles, CA 90089-0740, USA
[c] University of California Riverside, Department of Earth Sciences, 1242 Geology, Riverside, CA 92521, USA

Received 27 September 2005; accepted in revised form 6 June 2006

Abstract

We measured solid-phase Mo and U concentrations in marine sediments from the California, Mexico, Peru, and Chile margins to ascertain the behavior of Mo and U during early diagenesis in continental margin settings. At sites along the California, Mexico, and Peru margins where there are estimates of mass accumulation rates, authigenic U accumulation rates range from ~0–50 nmol m^{-2} day^{-1}. At the California and Mexico margin sites Mo accumulation rates range from 0 to 134 nmol m^{-2} day^{-1} whereas at the Peru margin site rates may be as high as 550 nmol m^{-2} day^{-1}. We observe relationships between metal accumulation rates and the delivery and burial rates of organic carbon (C_{org}). In the case of Mo there appears to be at least two relationships between metal accumulation rate and organic carbon burial. For most of the data presented in this manuscript, continental margin sediments have a Mo:C_{org} accumulation rate ratio of ~20 μmol mol^{-1}. This value is significantly lower, however, than those reported for anoxic basins ~100 μmol mol^{-1}, but is consistent with reported Mo:C_{org} rain ratios from Mexico margin sediment traps. In contrast to Mo, there appears to be a single U:C_{org} burial ratio of ~5 μmol mol^{-1}, which includes a range of environments from anoxic basins and open ocean sites. We interpret the relationships between metal accumulation and organic carbon to indicate that the reactions that govern authigenic metal accumulation are primarily sensitive to the delivery and burial of organic carbon in these particular settings. However, we note that any relationship between metal accumulation and organic carbon could be indirect. In the particular case of Mo, based on what is known about Mo geochemistry from the literature, it is possible that Mo authigenesis is coupled to sulfur cycling in many of the environments covered by this study, and that the observed association between Mo and organic carbon burial is a consequence of the coupling between carbon and sulfur burial. Using the observed relationships between Mo and C_{org} burial as well as constraints from the Mo isotope budget we estimate that continental margin sediments are an important sink for Mo. The magnitude of this sink (~0.4×10^8 mol y^{-1}, or larger) may be as much as one quarter of the oceanic removal term, and is likely to be larger than the modern anoxic basin sink.

1. Introduction

The ocean's carbon cycle plays an important role in climate evolution. The interactive processes of biological production and ocean-atmosphere gas exchange ultimately regulate atmospheric CO_2 concentrations. One of the important locations for ocean carbon cycling is along the ocean basin boundaries (e.g., Muller-Karger et al., 2005). It is here where interactions between the ocean and terrestrial biospheres create the fertile conditions necessary to stimulate high rates of carbon fixation. These high rates of carbon fixation result in continental margins being globally significant repositories for fixed carbon as well as being potentially rich archives of high-resolution oceanographic records.

This contribution focuses on the geochemistry of Mo and U in reducing continental margin sedimentary

* Corresponding author.
E-mail address: mcmanus@coas.oregonstate.edu (J. McManus).

0016-7037/$ - see front matter © 2006 Elsevier Inc. All rights reserved.
doi:10.1016/j.gca.2006.06.1564

environments of the eastern Pacific and the potential of these two transition metals to serve as proxies for the ocean's carbon cycle. The solubility of these two elements decreases under the reducing conditions commonly encountered within the upper few centimeters of ocean margin sediments. Because of this decrease in solubility, the presence or absence of these elements in sedimentary deposits has been interpreted as a signature for past reducing conditions. However, our understanding of these elements has yet to mature to the point where their quantitative utility is possible. One of the difficulties in exploiting these elements as proxies for past geochemical conditions derives from the fact that sedimentary reducing conditions may be controlled by two complementary or competing processes: low dissolved oxygen availability above the sediments and the delivery of reactive organic carbon to the seafloor. These two factors, which are also closely coupled, combine to create shallow oxygen penetration depths where diagenetic reaction zones (e.g., oxygen consumption, nitrate, Mn, and Fe reduction) can be spatially compressed to the point where they functionally overlap.

In this paper, we present solid-phase Mo and U data from a number of cores along the California, Mexico, Peru, and Chile margins. These data point to authigenic enrichments of Mo and U in a number of these oxygen deficient settings and show a relationship between Mo and U accumulation and the accumulation rate of organic carbon. Based on these data, as well as some recent constraints on the Mo isotope balance, we suggest that the accumulation rate of Mo in continental margin sediments may represent 25% of the total Mo burial.

2. Geochemical background

2.1. Molybdenum geochemistry

Mo is a biologically essential trace element (e.g., Howarth and Cole, 1985; Howarth et al., 1988a,b; Marino et al., 1990; Paulsen et al., 1991; Cole et al., 1993; Tuit et al., 2004; and others); however, unlike many bioactive elements, variations in its water column distribution are small (Morris, 1975; Collier, 1985; and also see Brewer, 1975; Calvert and Pedersen, 1993 and references therein). Consistent with its generally conservative ocean distribution, Mo has a high salinity-normalized dissolved concentration (~110 nM) (Morris, 1975; Collier, 1985) and a modern-ocean residence time of approximately 0.8 million years (Emerson and Huested, 1991; Colodner et al., 1995). Rivers serve as the dominant source term for Mo to the ocean; whereas oxic and anoxic marine sedimentary systems are believed to be the primary sinks (e.g., Bertine and Turekian, 1973; Brumsack and Gieskes, 1983; Brumsack, 1986; Emerson and Huested, 1991; Calvert and Pedersen, 1993; Colodner et al., 1995; Piper and Isaacs, 1995; Crusius et al., 1996; Helz et al., 1996; Nameroff, 1996; Morford, 1999; Morford and Emerson, 1999; Siebert et al., 2003; Anbar et al., 2004; and others). In the case of oxic sediments, where roughly half of the Mo is removed from the ocean (Bertine and Turekian, 1973; Morford and Emerson, 1999), Mo is scavenged in association with metal oxides. This scavenging is possibly associated with a speciation change from the dissolved MoO_4^{2-} to the particle reactive MoO_3 (Tossell, 2005). In reducing sediments Mo is taken up in the presence of HS^- (e.g., Bertine, 1972; Berrang and Grill, 1974; Shimmield and Price, 1986; Shaw et al., 1990; Emerson and Huested, 1991; Calvert and Pedersen, 1993, and references therein). Under these conditions, soluble Mo is converted to particle reactive thiomolybdates (e.g., $MoO_xS_{4-x}^{2-}$; Helz et al., 1996; Erickson and Helz, 2000; Zheng et al., 2000; Vorlicek and Helz, 2002; Vorlicek et al., 2004). Thiomolybdates are scavenged from solution via sulfidized organic material (e.g., Tribovillard et al., 2004) or via Mo capture by Fe–S phases (e.g., Helz et al., 1996; Erickson and Helz, 2000). Bostick et al. (2003) suggest that an important Mo sink is likely to be Mo–Fe–S cuboidal clusters on FeS_2. Zheng et al. (2000) postulate that there are two thresholds for Mo authigenesis; one where pore water sulfide concentrations reach concentrations exceeding 0.05 μM and a second where sulfide concentrations reach 100 μM. Under low sulfide conditions, these workers speculate that Mo uptake occurs in the presence of Fe, possibly in association with a Fe–S phase. Under high sulfide conditions, they propose that uptake may occur in the absence of dissolved Fe, possibly as a metal sulfide (e.g., MoS_4^{2-}). A prominent feature of the previous work is the potential importance of the paired iron and sulfur cycle on the removal of Mo from the ocean (also see Lyons et al., 2003; Tribovillard et al., 2004; Wilde et al., 2004; Algeo and Lyons, 2006). Germane to the present work, this cycling begins under the reducing conditions that are common near the sediment-water boundary on many continental margins.

2.2. Uranium geochemistry

Much like Mo, uranium exhibits conservative behavior within oxygenated ocean waters and has a modern-ocean residence time of ~0.5 million years (Ku et al., 1977; Cochran, 1982; Chen et al., 1986; Cochran et al., 1986; Dunk et al., 2002). U is present in seawater at a concentration of ~13 nM as a stable U (VI) carbonate complex (e.g., Ku et al., 1977; Chen et al., 1986). A small but variable fraction of the total oceanic U is associated with particulate organic carbon (e.g., Anderson et al., 1998). This association produces a correlation between particulate U and the organic carbon settling flux in a variety of oceanographic regimes and has led to the idea that U may serve as a proxy for organic carbon transport to the seabed (Anderson, 1982; Knauss and Ku, 1983; Kumar et al., 1995; Anderson et al., 1998; Zheng et al., 2002). Rivers are the dominant source of U to the oceans, and the pri-

mary removal mechanism for U is via uptake across the sediment-water boundary of reducing sediments, with removal in hydrothermal systems being of secondary importance (e.g., Anderson, 1987; Palmer and Edmond, 1989; Sarin et al., 1990; Barnes and Cochran, 1993; Church et al., 1996). In terms of the sedimentary removal pathway, it appears that for sedimentary conditions near those for conversion of Fe^{3+} to Fe^{2+}, soluble U (VI) is reduced, perhaps through microbial mediation, to insoluble U (IV) (e.g., Cochran et al., 1986; Anderson, 1987; McKee et al., 1987; Barnes and Cochran, 1990; Lovley et al., 1991; Lovley et al., 1993; Fredrickson et al., 2000; King et al., 2000; Chaillou et al., 2002; Sani et al., 2004). Because this reduction potential is typically achieved in close proximity to the sediment-water boundary in continental shelf and slope environments, these sediments have elevated U concentrations relative to oxic environments (Dorta and Rona, 1971; Mo et al., 1973; Veeh et al., 1974; Degens et al., 1977; Bloch, 1980; Yamada and Tsunogai, 1983/84; Anderson et al., 1989a,b; Calvert and Pedersen, 1993; Legeleux et al., 1994; Morford and Emerson, 1999; Dunk et al., 2002; Nameroff et al., 2002; and others).

3. Study sites

Our study sites are continental margin environments, which border the eastern Pacific boundary along the California, Mexico, Peru, and Chile margins (Fig. 1; Table 1). Oxygen deficient waters bathe the Central and Southern California margin bottom sediments that span water depths from 500 to 1500 m (e.g., Berelson and Hammond, 1986; McManus et al., 1997; and references therein). Our sites off Southern California include stations within the series of submarine basins of the California Borderlands region (e.g., Emery, 1960). Topography retards mixing of the basin waters with the surrounding seawater, thus alteration of these waters occurs through diagenesis resulting in these basins having lower oxygen contents than their surrounding environments (e.g., Berelson et al., 1987). One attraction of using these basins for geochemical work is that an extensive array of relevant data has already been published providing a fertile data base for geochemical characterization (e.g., Berelson et al., 1987; Berelson et al., 1996; Jahnke et al., 1990; Shaw et al., 1990; Reimers et al., 1992; Ingall and Jahnke, 1994; Reimers et al., 1996; and many others)

The stations along the Mexico margin have low bottom water oxygen concentrations of ~1 μM or less, high pore water NH_4 concentrations, and pore water depletions of sulfate (Berelson et al., 2005). The Soledad site is located within a 545 m deep basin with a sill depth of approximately 250 m (Silverberg et al., 2004); this basin is also discussed in Van Geen et al. (2003). The continental margin site off Mazatlan is located near that which has been studied previously (Ganeshram et al., 1999; Hartnett and Devol, 2003). The San Blas station lies within a 430 m deep silled basin with an approximate sill depth of 300 m. This site lies

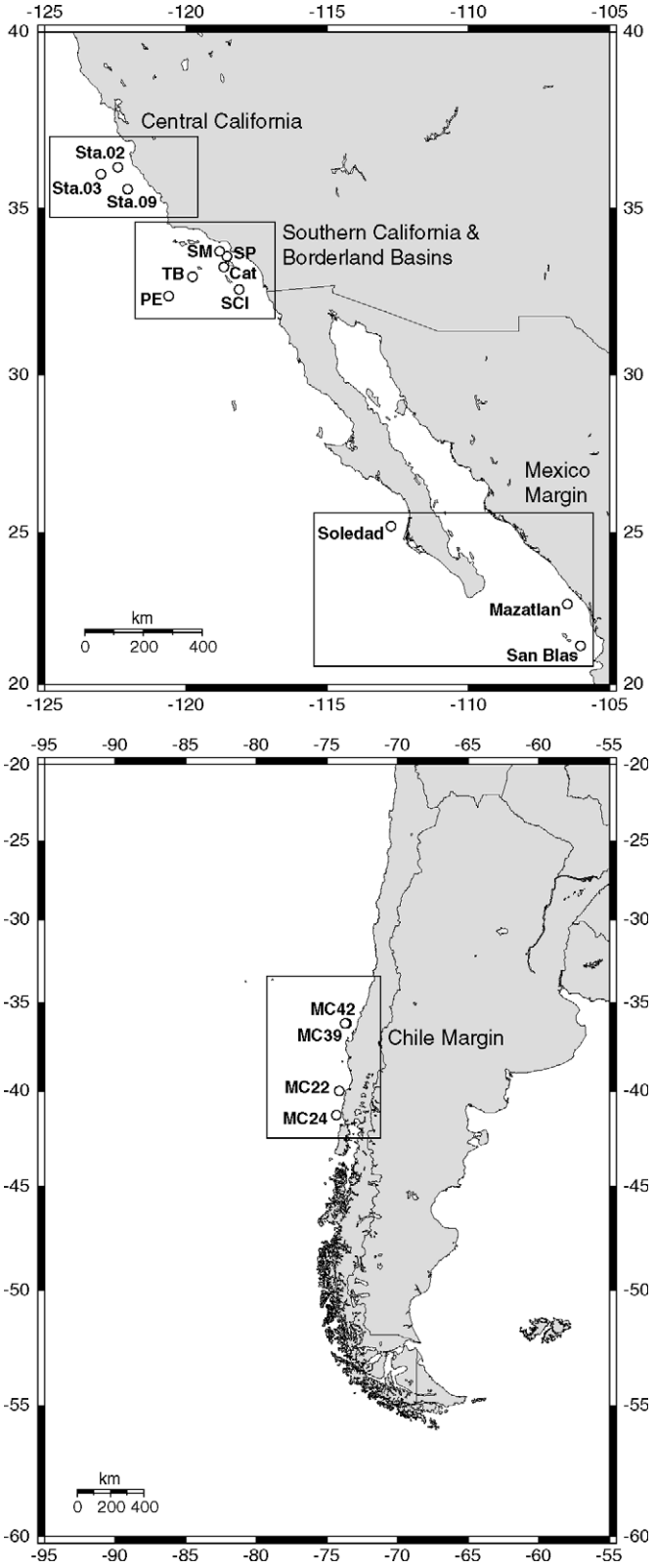

Fig. 1. Map of study areas showing approximate locations of sites used in this manuscript. Station abbreviations are: SM, Santa Monica Basin; SP, San Pedro Basin; Cat, Catalina Basin; SCl, San Clemente Basin; TB, Tanner Basin; and PE, Patton Escarpment. Other stations are as identified in Table 1.

Table 1
Study site characteristics

Sta. location notes	Depth (m)	Lat. (°N)	Long. (°W)	BW O_2[d] (μM)	C_{ox}[e] (mmol m^{-2} d^{-1})	MAR[f] (mg cm^{-2} y^{-1})
Central California Margin						
Sta. 02[a]	1455	36.2	122.4	53	2.4 ± 0.9	
Sta. 03[a]	3595	36.0	123.0	133	0.7 ± 0.4	
Sta. 09[b]	1500	35.56	122.05	56	1.1 ± 1.6	
Southern California Margin and Borderland Basins[a,b]						
Patton Escarpment	3707	32.4	120.6	132	0.4 ± 0.1	3
Tanner Basin	1514	33.0	119.7	27	1.0 ± 0.3	12
Catalina Basin	1300	33.3	118.6	19	1.3 ± 0.1	14
San Pedro Basin	896	33.5	118.4	3–8	1.8 ± 0.4	29
Santa Monica Basin	905	33.7	118.8	4–10	1.9 ± 0.2	16
San Clemente Basin	2053	32.6	118.1	52	1.0 ± 0.1	15
Mexican Margin[c]						
Mazatlan	442	22.67	106.48	0.2	>1.06	9
Soledad	542	25.21	112.72	0	>1.78	50
San Blass	430	21.26	105.96	0	>1.28	21
Chile Margin						
MC22	430	−40.0	74.1	148	*2.5 ± 1.2*	
MC24	246	−41.3	74.3	51	*8.3 ± 3.6*	
MC39	510	−36.2	73.6	63	*10.0 ± 4.1*	
MC42	1028	−36.2	73.7	70	*4.2 ± 1.9*	
Peru Margin						
MC82	264	−13.7	76.7	<10		*25*

Primary sources for cruise details and additional data include.

[a] Berelson et al. (1996) and McManus et al. (1997).

[b] Hammond et al. (2004).

[c] Mexican margin sites are discussed in Berelson et al. (2005) and in Poulson et al. (2006).

[d] BW is Bottom Water. Ranges are the values based on multiple visitations[1,2]. Values in italics do not have bottom water O_2 concentrations. Values are estimates based on the CTD dissolved oxygen value (lower value) and our estimate of the deep water offset (5–9 μM), based on bottle calibrations from other locations during the same cruise. The higher value is a maximum based on the maximum observed offset and the most likely oxygen concentration lies between the two values.

[e] C_{ox} is the organic carbon oxidation rate and is calculated from the evolution of respiratory CO_2 during the course of the incubations with the exception of the Peru/Chile cores, see Berelson et al. (1996) and Berelson et al. (2005) for further details. Data from the Chile margin cores are based on the sum of the pore water dissolved oxygen fluxes and the dissolved nitrate fluxes (i.e., oxygen and nitrate sedimentary uptake rates). Borderland basin C_{ox} values are averages of multiple visitations from our group (Berelson et al., 1996; McManus et al., 1997; Hammond et al., 2004), with the exception of the San Pedro Basin which is based on a single visitation (Berelson et al., 1996).

[f] Mass accumulation rates (MAR) were compiled for the Borderland basins by Berelson et al. (1996). The Mexican margin mass accumulation rates are from Poulson et al. (2006) and are the same sites reported here. Data from the Peru margin are from this study and are italicized because of the added uncertainty imposed on the data by a non-steady state distribution of $^{210}Pb_{xs}$ as discussed in the text.

Table 2
Reference materials for Mo and U (value reported in μg g^{-1} solid)

Standard	Mo	±	*n*	Ref.	M/R	U	±	*n*	Ref.	M/R
BCR-1	1.64	0.06	13 (5)	1.54	1.06	2.0		1	1.8	1.16
MAG-1	1.14	0.08	11 (5)	1.17	0.97	2.5	0.2	3 (3)	2.7	0.93
AGV-1	2.4	0.1	7 (3)	2.1	1.14					
W-2	0.47	0.03	7 (3)	0.44	1.07					

Standards are as described for Appendix A. *n* is the number of individual sample analyses that comprise each value where the number in parentheses is the number of individually weighed and digested samples. When the two numbers differ it means that an individual sample was rerun on a different day and that number was also used to compute the average value. When the two numbers are the same it means that each individually digested sample was only run on one occasion. M/R is the measured value divided by the reported or literature or reference value. For Mo a more up to date review is given in Wieser and DeLaeter (2000).

landward of the Tres Marias Island chain. Oxygen penetration into the sediments along the Chile margin ranges from <1 mm to ~3 cm (McManus et al., 2003), and these sites generally have higher bottom water oxygen concentrations than observed in the other regions discussed here. Consistent with their relatively shallow oxygen penetration depths these sites have enriched pore water ammonium concentrations within the upper ~2 cm, but dissolved sulfate concentrations are not significantly different from seawater (McManus, unpublished data). The Peru margin site lies at approximately 250 m water depth below the perennial Peru upwelling system and is an organic carbon rich (~14% organic carbon) site. This site has low bottom water oxygen concentrations (<10 μM), and this region in general is known for its high organic carbon contents, high solid-phase sulfur concentrations, rapid sediment accumulation rates, and high authigenic metal concentrations (e.g., see Böning et al., 2004). Additional data for both the Chile margin sites and the Mexico margin sites are reported elsewhere (McManus et al., 2003; Berelson et al., 2005; Poulson et al., 2006). We note that oxygen concentrations vary temporally in Northeastern Pacific bottom waters and this adds some uncertainty (~5 μM) regarding our choice of this value for all sites (Scholkovitz and Gieskes, 1971; Reimers et al., 1990; Berelson, 1991).

4. Methods

Sediment cores were collected using a multiple corer (abbreviated MC in site locations; Barnett et al., 1984). ^{210}Pb was determined by γ-ray spectroscopy (e.g., Gilmore and Hemingway, 1995), and the details of sediment processing are presented elsewhere (e.g., Wheatcroft and Sommerfield, 2005). Organic carbon was measured by difference, using an elemental analyzer for total carbon determination and a coulometer with acidification module for total inorganic carbon. Organic carbon is then calculated as the difference between the total and inorganic carbon (Hedges and Stern, 1984). For a subset of samples, acidification was done to remove the inorganic carbon prior to the determination of organic carbon (Verardo et al., 1990). Each approach provides consistent results with average sample reproducibility for the entire data set of ±0.05%C. This value is based on the reproducibility of >70 samples having repeat determinations. Dissolved oxygen was measured using a standard Winkler or micro-Winkler technique (e.g., Carpenter, 1965).

For solid-phase metal analyses we typically digest 25–100 mg of dry ground sediment using a series of HF, HNO_3, and HCl digestions on a hot plate or using a microwave digestion technique (CEM, MARS 5000). Analyses were done using ICP-MS (Mo and U) or ICP-AES (Al, Ti, and Mn). To evaluate the compatibility of the two techniques we compared the hot plate and microwave-assisted digestion techniques along with an alkaline fusion technique (e.g., Murray et al., 2000). This comparison was accomplished by analyzing standard reference materials in duplicate or triplicate using each technique (U.S.G.S. reference materials BCR-1, AGV-1, W-2, and MAG-1). These data generally show agreement among the techniques and with the reported value (e.g., Potts et al., 1992). In addition to these standard reference materials, we also digested a number of internal laboratory samples including a carbonate rich sediment, a carbonate poor marine sediment, and a sediment trap sample from 1750 m depth along the California–Oregon continental margin, and these data also suggest excellent reproducibility among the techniques (Appendix A).

We also analyzed a number of standard reference materials for Mo and U (Table 2). Agreement with the reported values is typically within 16% or better. In the case of Mo we also digested 40 samples with concentrations ranging from 1 to 30 ppm using a double-isotope dilution technique (e.g., Siebert et al., 2001) and compared those results with the results obtained from other digestion techniques. The average difference between these results is 8%. The precision of each analysis is generally superior to the agreement with the standard reference materials indicating that each technique provides internally consistent results. None of these comparisons assures absolute accuracy of all results, but these comparisons do suggest internally consistent results. Furthermore, the natural variability discussed within this manuscript is typically larger than any of the uncertainties associated with the reproducibility or accuracy of our results.

5. Results

Excess ^{210}Pb was determined on one core from the Peru margin, and those data were used to estimate the linear sedimentation rate and the mass accumulation rate (Fig. 2). These data show a distinct layer of well-mixed

sediment from ~3 to 5 cm depth. We interpret these data as emplacement of a uniform sediment pulse, perhaps as a debris flow or some other non-steady state phenomenon. To calculate a linear sedimentation rate we excluded those data and calculated the rate above and below the event (Fig. 2). The calculated sedimentation rates derived from the data above and below the uniform horizon are indistinguishable and we use the average of all the data to calculate the sedimentation rate for this site. We recognize that this particular site harbors some additional uncertainty with respect to its sedimentation rate and we are cautious about any strict interpretations regarding that rate. We note, however, that the sedimentation rate (0.08 cm yr^{-1}) is within the range of previous work in this region (e.g., 0.03–1.2 cm yr^{-1} in Reimers and Suess, 1983).

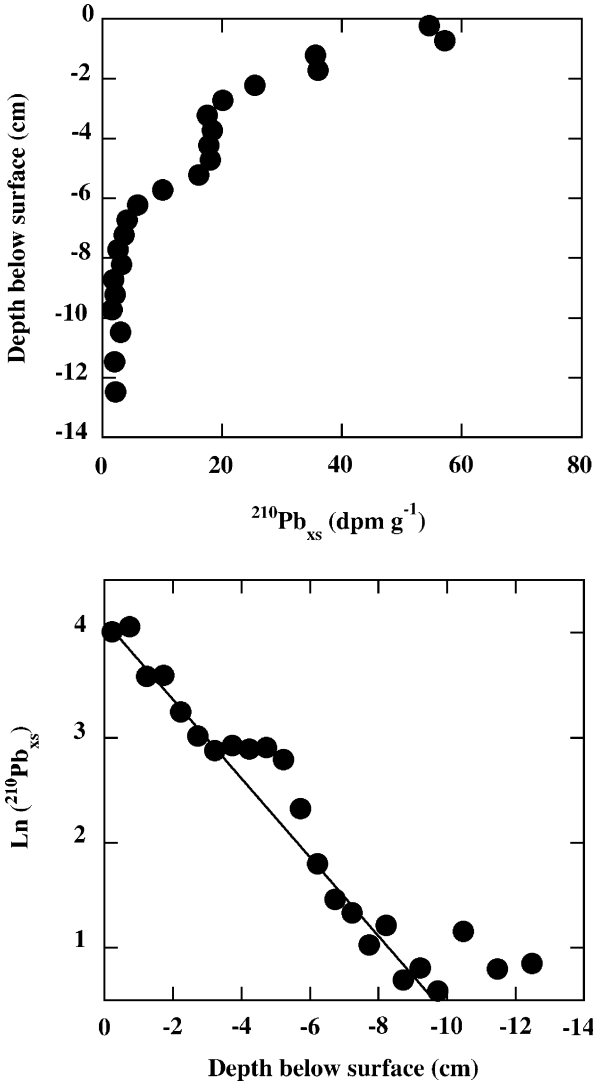

Fig. 2. $^{210}Pb_{xs}$ plotted as a function of depth (top) and ln $^{210}Pb_{xs}$ as a function of depth (bottom). Data are for a companion core collected during the same deployment as the solid-phase concentration data reported here. Supported ^{210}Pb is calculated from ^{214}Pb data and subtracted from the total ^{210}Pb. The slope in the ln $^{210}Pb_{xs}$ as a function of depth allows us to calculate the linear sedimentation rate from the relation $\ln A_z = \ln A_0 - (\lambda/w)z$, where A is $^{210}Pb_{xs}$, w is the linear sedimentation rate and z is depth in the sediment.

Site averaged organic carbon distributions vary from <2 to >14% (Table 3, Fig. 3). For many sites, organic carbon distributions decrease with depth, consistent with a decrease in organic carbon driven by diagenesis of reactive organic material, but this pattern is not always observed.

We present the authigenic solid-phase data as the metal to Al ratio (Figs. 4–7). The dashed lines in each panel represent what we believe to be the siliciclastic "background" metal to Al ratio. Our choice for the Mo:Al background is based, in part on the determination of minimum Mo:Al ratios for cores from each region (e.g., Sta. 09 and 22MC). Data from several sites along the central California margin and the Chile margin range between 8 and 14×10^{-6} and for our purposes we selected the middle value (also see Siebert et al., 2006). These values coincide with the values for igneous rocks and sandstones (e.g., range $6–19 \times 10^{-6}$ as reported in Turekian and Wedepohl, 1961). This background value has been used elsewhere, and is supported by Mo isotope work in the Santa Monica and San Pedro basins as well as the Mexico margin sites discussed here (Poulson et al., 2006). These authors use a Mo:Al ratio of 11×10^{-6} for the lithogenic dilution of the authigenic Mo isotope signature. In the case of U we adopt a lithogenic U:Al ratio of 18×10^{-6}. This value is similar to that of basalt, sandstones, and deep-sea clays, and is smaller than shale (e.g., Turekian and Wedepohl, 1961). From these lithogenic ratios we calculate an authigenic metal concentration (Table 3).

The central California sites (Fig. 4) and the Chile margin sites (Fig. 5) are generally less enriched in Mo than the Southern California, Mexico, and Peru margin sites. Many of these sites exhibit down-core metal to Al ratio increases with depth, with the enrichments generally occurring shallower for U than for Mo. From a diagenetic perspective the Chile margin sites are quite similar to the central California margin sites having moderately shallow oxygen penetration depths, small dissolved sulfate gradients and ammonium distributions characteristic of continental margin diagenesis (see McManus et al., 2003 for oxygen profiles).

The Southern California borderlands region (Fig. 6) includes two sites (San Clemente Basin and the Patton Escarpment) where there are significant near-surface solid-phase Mn enrichments. While the Mn enrichments for these sites do not appear to influence the distribution of solid-phase U, Mo is enriched in the Mn-rich zone (Fig. 6). Below this zone Mo:Al ratios are near the lithogenic background, with a slight increase at depth below ~15 cm. In the case of the remaining Southern California sites, each exhibits significant enrichment over the lithogenic value with Tanner Basin having the greatest enrichment (note the change in scale for the Tanner Basin site) whereas San Pedro and Santa Monica Basins both show the highest concentrations at shallow depths. Catalina and Tanner Basins each show a general increase with depth in both metals.

The Mexico and Peru margin sites (Fig. 7) have the greatest metal enrichments. The Mexico margin sites tend to have higher organic carbon contents than the Southern

Table 3
Sediment data

Station	Depth (cm)	Mo (μg g^{-1})	U (μg g^{-1})	U/Mo (g g^{-1})	Corg%	Al%	Mn (μg g^{-1})	Mo (a) (μg g^{-1})	U (a) (μg g^{-1})
Sta. 02	0.25	1.34	2.99	2.2		6.11	357	*0.75*	*2.19*
	1.50	1.58	3.54	2.2		6.18	324	*0.90*	*2.43*
	3.50	1.62	4.03	2.5		6.23	337	*0.93*	*2.91*
	5.00	1.64	3.99	2.4		6.44	343	0.93	2.83
	7.50	1.24	3.95	3.2		6.43	348	0.53	2.80
	10.50	1.25	4.98	4.0		6.32	341	0.55	3.84
	13.50	1.50	5.34	3.6		6.24	334	0.81	4.21
	16.50	2.11	5.27	2.5		6.24	340	1.42	4.15
	20.00	2.38	5.47	2.3		6.23	347	1.69	4.35
	22.00	2.06	4.96	2.4		6.13	336	1.39	3.86
Average				**2.73**				**1.05**	**3.72**
±				**0.62**				**0.46**	**0.65**
Sta. 03	0.25	0.89	2.62	3.0		6.40	456	*0.16*	*1.64*
	1.50	0.87	2.88	3.3		6.28	346	*0.18*	*1.75*
	3.50	0.84	3.08	3.6		6.70	307	*0.11*	*1.87*
	5.00	1.00	4.22	4.2		6.34	302	0.30	3.08
	7.00	1.09	4.47	4.1		6.56	306	0.37	3.29
	9.50	1.05	3.97	3.8		6.74	301	0.31	2.76
	12.50	1.50	5.07	3.4		6.71	319	0.76	3.86
	15.50	1.69	5.92	3.5		6.48	346	0.97	4.75
	18.50	1.74	6.16	3.5		6.63	451	1.01	4.96
Average				**3.60**				**0.62**	**3.78**
±				**0.40**				**0.34**	**0.91**
Sta. 09	0.21	0.22	0.86	4.0		1.60	57	*0.04*	*0.58*
	1.47	0.22	0.93	4.3		1.55	57	*0.05*	*0.65*
	3.97	0.21	0.87	4.2		1.57	46	*0.03*	*0.58*
	7.97	0.19	0.95	4.9		1.73	50	0.00	0.63
	11.97	0.27	1.31	4.8		2.30	75	0.02	0.90
	17.97	0.28	1.32	4.7		2.42	76	0.02	0.88
Average				**4.48**				**0.01**	**0.81**
±				**0.39**				**0.01**	**0.15**
22MC	0.17	0.86	1.85	*2.2*	1.59	8.28	740	*−0.05*	*0.36*
	0.52	0.85	1.88	*2.2*	1.58	8.29	734	*−0.06*	*0.39*
	1.74	0.94	2.63	*2.8*	1.59	8.39	745	0.02	1.12
	7.51	1.11	3.55	3.2	1.38	8.39	737	0.19	2.04
	10.90	0.92	2.82	3.1	1.49	8.42	745	−0.01	1.31
	14.29	1.61	5.57	3.5	1.31	8.47	708	0.67	4.04
Average				**3.25**	**1.49**			**0.22**	**2.13**
±				**0.20**	**0.12**			**0.32**	**1.34**
24MC	1.00	1.16	2.76	2.4	2.73	7.34	602	*0.35*	*1.43*
	3.00	1.19	2.72	2.3	2.71	7.38	593	*0.38*	*1.39*
	5.00	1.15	2.80	2.4		7.26	606	0.35	1.49
	7.00	1.14	2.98	2.6	2.22	7.18	612	0.35	1.69
	9.00	1.21	2.90	2.4	2.26	7.16	616	0.42	1.61
	11.00	1.30	2.95	2.3	1.78	7.38	685	0.49	1.62
	13.00	1.37	3.52	2.6	1.26	7.56	725	0.54	2.15
	17.00	1.42	4.69	3.3	1.24	7.71	726	0.57	3.31
	21.00	1.45	3.96	2.7	0.89	7.83	759	0.59	2.55
	23.00	1.38	3.16	2.3	1.05	7.80	765	0.53	1.75
Average				**2.53**	**1.79**			**0.48**	**2.02**
±				**0.31**	**0.71**			**0.10**	**0.63**
39MC	0.21	1.36	2.58	1.9		8.45	501	*0.43*	*1.06*
	0.63	1.45	2.57	1.8		8.44	490	*0.52*	*1.05*
	1.88	1.41	2.90	2.1	2.34	8.39	498	*0.49*	*1.39*
	3.26	1.60	3.47	2.2	2.44	8.55	497	*0.66*	*1.93*
	5.65	2.00	3.78	1.9	2.42	8.54	497	1.06	2.24
	9.04	2.12	3.73	1.8	2.50	8.72	507	1.16	2.16
	15.82	2.25	4.00	1.8	2.34	8.51	498	1.32	2.47
	19.21	2.11	4.22	2.0	2.03	8.43	517	1.18	2.70
Average				**1.92**	**2.35**			**1.18**	**2.39**
±				**0.15**	**0.17**			**0.11**	**0.24**

(*continued on next page*)

Table 3 (*continued*)

Station	Depth (cm)	Mo (μg g^{-1})	U (μg g^{-1})	U/Mo (g g^{-1})	Corg%	Al%	Mn (μg g^{-1})	Mo (a) (μg g^{-1})	U (a) (μg g^{-1})
42MC	0.73	1.37	2.55	1.9	2.94	8.13	487	*0.48*	*1.09*
	2.01	1.37	2.93	2.1	2.93	8.25	497	*0.46*	*1.44*
	5.10	1.57	3.24	2.1	3.02	8.24	493	0.66	1.76
	5.79	1.53	3.03	2.0	2.81	8.23	490	0.62	1.55
	14.57	1.78	3.79	2.1	2.45	8.24	520	0.88	2.31
	17.96	1.78	3.43	1.9	2.50	8.11	526	0.89	1.97
	18.65	1.68	3.42	2.0	2.35	8.11	528	0.79	1.96
Average				**2.02**	**2.72**			**0.77**	**1.91**
±				**0.10**	**0.27**			**0.12**	**0.28**
82MC	0.52	70.08	17.34	0.2	16.27	2.27	114	69.83	16.93
	1.04	69.54	18.73	0.3	16.40	2.44	125	69.27	18.29
	1.74	74.02	22.36	0.3	15.67	2.51	130	73.74	21.91
	2.43	79.24	24.54	0.3	15.84	2.57	131	78.96	24.07
	4.82	88.08	22.95	0.3	14.70	2.45	126	87.81	22.51
	8.21	82.66	19.19	0.2	13.42	2.22	116	82.42	18.79
	11.60	87.71	18.70	0.2	13.64	2.41	123	87.45	18.26
	14.99	67.64	21.08	0.3	12.29	2.20	110	67.40	20.69
	15.68	66.57	18.59	0.3	12.54	2.42	121	66.31	18.15
	18.38	77.20	14.17	0.2	14.68	3.15	155	76.85	13.60
	19.07	71.37	14.52	0.2	14.82	2.97	148	71.04	13.98
Average				**0.26**	**14.57**			**75.55**	**18.83**
±				**0.04**	**1.44**			**7.75**	**3.31**
Mazatlan	1.00	6.26	4.29	0.7		6.22	219	5.57	3.17
	3.75	8.85	11.10	1.3		7.13	244	8.07	9.82
	9.25	10.06	13.30	1.3		7.12	249	9.27	12.02
	14.75	9.36	10.94	1.2	8.18	7.09	255	8.58	9.66
	20.25	12.02	17.19	1.4	8.73	4.21	251	11.55	16.43
	25.75	11.06	10.65	1.0	7.56	6.00	244	10.40	9.57
	31.25	12.61	10.80	0.9	8.09	7.37	271	11.80	9.47
	36.75	14.33	13.09	0.9	8.33	3.55	245	13.94	12.45
	42.25	14.33	11.66	0.8	8.09	3.67	256	13.93	10.99
	47.75	16.80	12.19	0.7	7.19	3.97	248	16.36	11.48
	53.25	15.77	12.51	0.8	7.75	5.29	247	15.19	11.56
	59.00	16.57	17.32	1.0	8.30	5.49	249	15.96	16.33
Average				**1.00**	**8.03**			**11.72**	**11.08**
±				**0.25**	**0.46**			**3.44**	**3.44**
San Blass	0.15	4.96	3.04	0.6		4.79	174.5	4.44	2.18
	1.15	5.86	5.36	0.9	5.89	6.20	209.2	5.18	4.25
	3.75	9.19	11.89	1.3	7.01	7.16	227.4	8.40	10.60
	9.25	8.33	9.49	1.1	6.39	7.44	230.3	7.51	8.15
	15.00	9.78	14.15	1.4	6.46	7.28	233.8	8.98	12.84
	26.75	11.86	12.25	1.0	7.31	6.99	254.8	11.09	11.00
	38.25	15.88	11.99	0.8	6.54	7.22	271.3	15.09	10.70
	47.75	12.03	11.32	0.9	6.82	7.15	280.6	11.25	10.04
Average				**1.02**	**6.63**			**8.99**	**8.72**
±				**0.27**	**0.46**			**3.47**	**3.67**
Soledad	1	4.16	6.78	1.6	7.09	3.77	175.4	3.75	6.10
	4	5.26	8.45	1.6	7.34	4.00	186.4	4.82	7.73
	9.75	6.70	8.32	1.2	7.25	3.96	185	6.27	7.61
	15.25	17.82	9.50	0.5	7.67	3.77	173.5	17.41	8.83
	20.75	8.02	10.58	1.3	7.55	4.15	185.7	7.56	9.83
	26.25	8.13	9.27	1.1	7.07	4.10	181.4	7.68	8.53
	31.75	9.53	10.99	1.2	7.63	3.74	171.1	9.12	10.32
	37.25	8.35	10.68	1.3		3.81	171.3	7.93	9.99
	42.75	10.27	9.99	1.0	6.97	3.76	171.6	9.85	9.31
	46.5	18.82	10.29	0.5	7.79	3.93	179.1	18.38	9.58
Average				**1.14**	**7.37**			**9.28**	**8.78**
±				**0.38**	**0.30**			**4.90**	**1.31**
San Clemente	0.75	37.34	2.75	0.1		6.00	30196	*36.68*	*1.67*
	2.50	10.10	2.42	0.2		6.08	19717	*9.43*	*1.32*
	5.00	0.85	2.08	2.5		6.25	2343	*0.16*	*0.96*
	10.50	0.50	3.62	7.2	3.41	5.95	3019	− 0.15	*2.54*
	16.50	0.75	4.11	5.5		6.36	1149	0.05	2.96

Table 3 (*continued*)

Station	Depth (cm)	Mo (μg g^{-1})	U (μg g^{-1})	U/Mo (g g^{-1})	Corg%	Al%	Mn (μg g^{-1})	Mo (a) (μg g^{-1})	U (a) (μg g^{-1})
42MC	0.73	1.37	2.55	1.9	2.94	8.13	487	*0.48*	*1.09*
	24.00	0.92	5.09	5.5		6.20	3558	0.24	3.98
Average								**0.14**	**3.47**
±								**0.14**	**0.72**
Catalina	2.5	1.50	2.68	*1.8*	5.24	6.21	385.7	*0.82*	*1.56*
	8	1.75	5.56	3.2	3.72	6.27	394.5	1.06	4.43
	10.5	1.80	4.86	2.7	4.32	5.91	372.4	1.15	3.80
	16.5	2.08	5.87	2.8	3.72	6.13	381.8	1.40	4.77
	19.5	2.10	8.26	3.9		6.21	370	1.41	7.14
	19.5	2.13	7.81	3.7		6.02	360	1.47	6.73
	23	2.25	7.87	3.5		6.24	374.9	1.57	6.75
	23	2.45	7.86	3.2	2.31	6.21	369.3	1.77	6.74
Average				**3.29**	**3.86**			**1.40**	**5.77**
±				**0.44**	**1.07**			**0.24**	**1.38**
San Pedro	1.50	7.13	7.27	1.0	5.08	6.32	347	*6.43*	*6.14*
	3.50	3.57	3.41	1.0	4.08	7.20	411	*2.78*	*2.12*
	6.00	3.49	3.64	1.0	4.20	7.10	403	2.71	2.36
	10.50	3.84	5.28	1.4	4.32	6.85	395	3.09	4.04
	14.50	3.41	4.32	1.3	3.72	7.13	402	2.62	3.04
	22.00	3.17	4.85	1.5		7.17	400	2.38	3.56
	26.00	3.30	4.33	1.3	3.46	7.39	440	2.48	3.00
	30.00	3.13	4.50	1.4	2.31	7.29	417	2.33	3.19
Average				**1.24**	**3.88**			**2.60**	**3.20**
±				**0.21**	**0.86**			**0.28**	**0.57**
Santa Monica	0.75	5.27	6.74	1.3	5.15	5.67	342.5	*4.65*	*5.72*
	2.5	7.96	9.24	1.2	4.92	6.90	393.7	*7.20*	*8.00*
	5	4.86	6.61	1.4	3.96	6.38	344.6	4.16	5.46
	10.5	4.80	7.38	1.5	3.90	5.92	312.5	4.15	6.31
	16.5	4.26	4.55	1.1	2.28	7.35	362.7	3.45	3.22
	24	5.60	5.19	0.9	4.36	6.46	336.3	4.89	4.03
Average				**1.22**	**4.09**			**4.16**	**4.76**
±				**0.22**	**1.02**			**0.59**	**1.39**
Patton Escarpment	0.50	15.29	2.37	0.2	1.26	6.91	8130	14.52	1.13
	2.50	11.96	2.40	0.2	1.28	7.04	8503	11.19	1.13
	5.00	1.46	2.27	1.6	1.19	6.53	2658	0.75	1.10
	9.00	0.73	2.10	2.9	0.85	6.38	829.6	0.03	0.95
	13.00	0.52	2.71	5.2	1.00	6.39	525.9	−0.19	1.02
Average					**1.12**				**1.07**
±					**0.19**				**0.08**
Tanner Basin	0.75	2.35	3.07	1.3	7.27	3.04	139.4	*2.01*	*2.52*
	2.50	3.50	7.91	2.3	6.48	3.23	140.9	*3.14*	*7.33*
	5.00	4.54	7.65	1.7	6.48	3.24	146.1	*4.18*	*7.07*
	10.50	4.00	7.93	2.0	5.61	3.52	155	3.61	7.29
	17.50	5.02	7.35	1.5	6.13	3.35	151.7	4.65	6.74
	24.50	7.10	10.06	1.4	6.67	3.26	143.1	6.74	9.47
Average				**1.69**	**6.44**			**5.00**	**7.84**
±				**0.37**	**0.55**			**1.59**	**1.44**

(a) indicates the calculated authigenic concentration. Average values are generally those from below the depth where both metals appear to be undergoing reducing authigenesis. In locations where this depth is clearly too shallow (i.e., Patton Escarpment), we chose a deeper starting value. We also chose shallower starting depths for sites where authigenesis appears to have begun shallower in the sediment column (e.g., Mexican margin), and excluded those values that appear to have a significant Mn-rich zone. Bold font indicates average and ± values.

California margin, but there is some overlap (Table 3). The Peru margin site has the highest organic carbon concentration and has the greatest enrichment of Mo and U of any of the sites presented here. Because of the high organic carbon contents coupled with the low bottom water oxygen content, the Peru margin site is considered to be the most reducing of the sites presented.

6. Discussion

6.1. Comparisons between Mo and U geochemistry

At the Central California and Chile margins, which represent the least oxygen-depleted regions discussed here, there are sites with essentially no Mo enrichment above

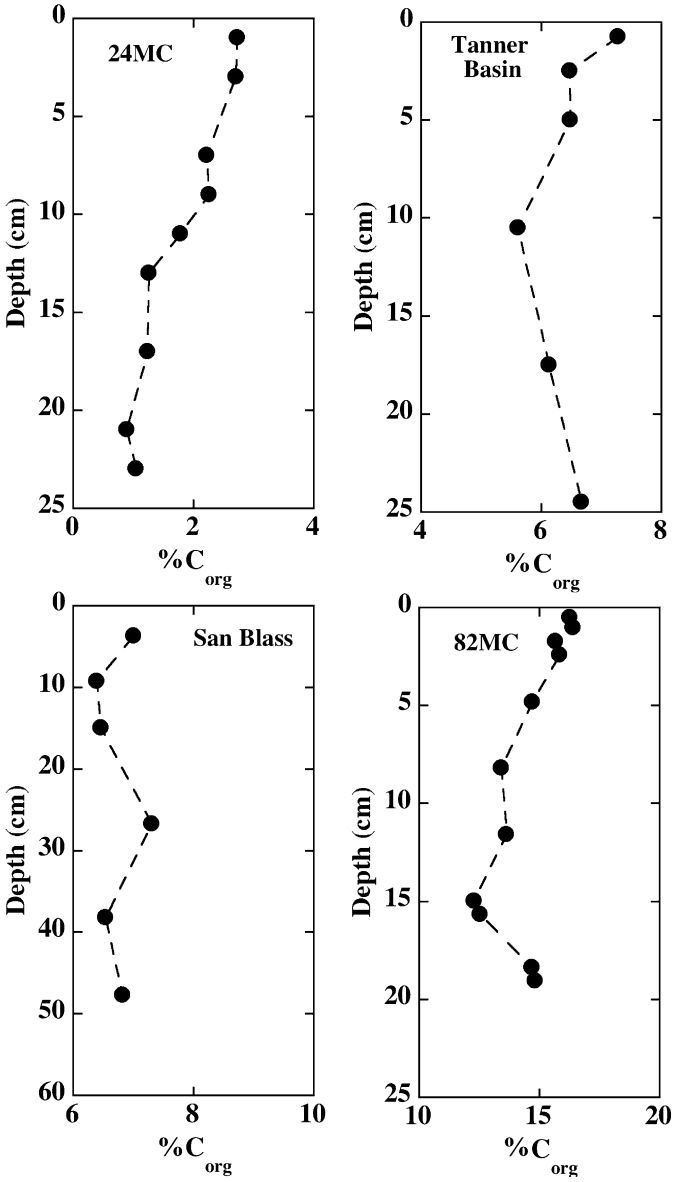

Fig. 3. Organic carbon contents of representative cores from this study plotted as a function of sediment depth. The complete data set is reported in Table 3.

background and only minor enrichments in solid-phase U. In addition, for some sites there appears to be some diagenetic separation between U and Mo, with the Mo enrichment lagging that of the U enrichment (Figs. 4 and 5). Likewise, the Catalina and Tanner Basins of Southern California show authigenic metal enrichments with there being at least a suggestion that Mo authigenesis is lagging that of U (Fig. 6). The data resolution are insufficient to fully support the contention of diagenetic separation, however, it does appear that the patterns of U and Mo in those cores are slightly different from the more reducing sites.

For both San Pedro and Santa Monica Basins, the two most reducing of the southern California sites, Mo exhibits no apparent diagenetic separation from U with authigenesis ensuing near the sediment-water boundary (Fig. 5). The near-surface uptake of U is consistent with pore water U data, which exhibit an exponential decrease in concentration from the bottom water value to approximately 3–5 cm depth (McManus et al., 2005). For Mo, its association with organic matter or metal oxides can result in near-surface Mo release followed by removal in the presence of reduced sulfur, which is generated during early diagenesis (also see Shaw et al., 1990 and McManus et al., 2002). There is also no diagenetic separation between U and Mo at the more carbon rich sites of the Mexico and Peru margins, and in general the enrichment of Mo becomes greater (i.e., the U:Mo ratio decreases) with increasing organic carbon contents. We speculate that this latter observation may be related to higher reduced sulfur contents at the more organic rich sites (e.g., Böning et al., 2004). This idea is consistent with previous work on the Mo association with sulfur (Section 2.1, also see Böning et al., 2004) and is consistent with Mo being highly enriched in sulfide-rich marine basins (e.g., Algeo and Lyons, 2006).

Several sites from this study also exhibit an increase in metal enrichment with depth, but not always. Along the central California margin and the Chile margin, where authigenic enrichments are quite small, the kinetics of metal authigenesis may be sufficiently slow that authigenesis occurs over the scale of several centimeters leading to authigenic enrichments that increase with depth (see similar discussion by Sundby et al., 2004). This interpretation is one possibility for an increase in solid-phase concentration with depth, i.e., that authigenic Mo enrichment continues long after burial and several centimeters into the sediments. This interpretation has been favored in the estuary and Gulf of St. Lawrence (Sundby et al., 2004) and in the Bay of Biscay (Chaillou et al., 2002). However, it is also possible that authigenic metal accumulation is decreasing with time (i.e., the sediments are not at non-steady state with respect to authigenesis). We suspect that both of these processes are operative along continental margins. If kinetic considerations were the sole cause of the patterns observed, then we would expect to observe gradual increases in metal enrichment with depth everywhere, which is not the case. We propose that in locations where the sediment accumulation rate, organic carbon burial, and organic carbon recycling rate are sufficiently high, the reactions that drive authigenesis will occur within a few centimeters or less of the sediment-water boundary and that increases in concentration with depth are a result of temporal variations in authigenesis. At these particular sites there will also be little separation between U and Mo enrichment patterns in accordance with the condensed metal enrichment patterns previously observed for other authigenic metal enrichments (Shaw et al., 1990). What we mean by "high" here is not clear as we simply do not have sufficient data to identify those diagenetic boundaries. However, the Santa Monica, San Pedro, Mexico, and Peru sites are all likely in this category.

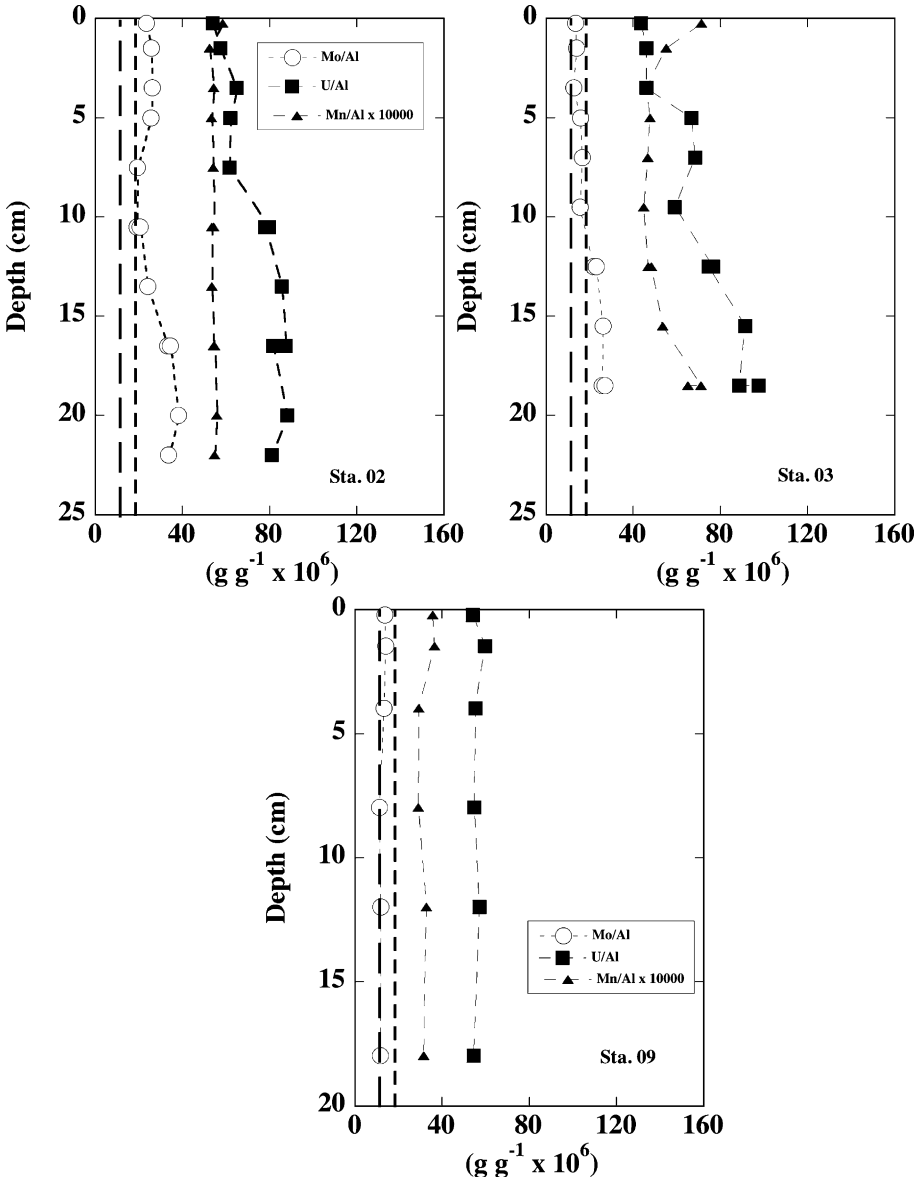

Fig. 4. Solid-phase distributions of Mo/Al, U/Al, and Mn/Al from central California. Units for Mo and U to Al ratios are as noted along the axis whereas for Mn it is g g^{-1} multiplied by the value listed in the legend. The dashed lines represent the Mo:Al and U:Al ratios used as background correction.

6.2. Relationships between organic carbon and authigenic metal accumulation

One of the primary issues regarding the potential utility of these elements as proxies for reducing conditions is that reducing conditions in marine settings can be fostered by two factors, low bottom water oxygen, and high organic carbon flux. It has been previously suggested that the U accumulation rate (U_{AR}) is sensitive to organic carbon delivery to the seabed (e.g., Anderson et al., 1989a,b; Rosenthal et al., 1995; Anderson et al., 1998; Chase et al., 2001; Zheng et al., 2002; and others). Likewise, it has been suggested that the influence of bottom water oxygen concentration on U_{AR} is of secondary importance as compared to the flux of reactive organic material if the organic flux exceeds a critical value above ~0.5 mmol C_{org} m^{-2} day^{-1} (McManus et al., 2005). This expectation is captured in the data from the Southern California and Mexico margins as well as from the compiled existing data (Fig. 8; Table 4). The fact that we do not observe multiple relationships between organic carbon delivery to the seafloor (C_{rain}) and U_{AR} (Figs. 8A and B) implies that the chemical mechanism(s) that govern U_{AR} are relatively insensitive to the changes in sediment pore fluid chemistry that occur as pore fluids progress from having oxygen present (e.g., Equatorial Pacific) to being sulfidic (e.g., Black Sea).

In the case of Mo, although there is less data available than for U, there also appears to be a relationship between organic carbon (C_{org}) rain rate and the Mo accumulation rate (Mo_{AR}), but the minimum flux of organic carbon to the seabed required for Mo authigenesis seems higher than

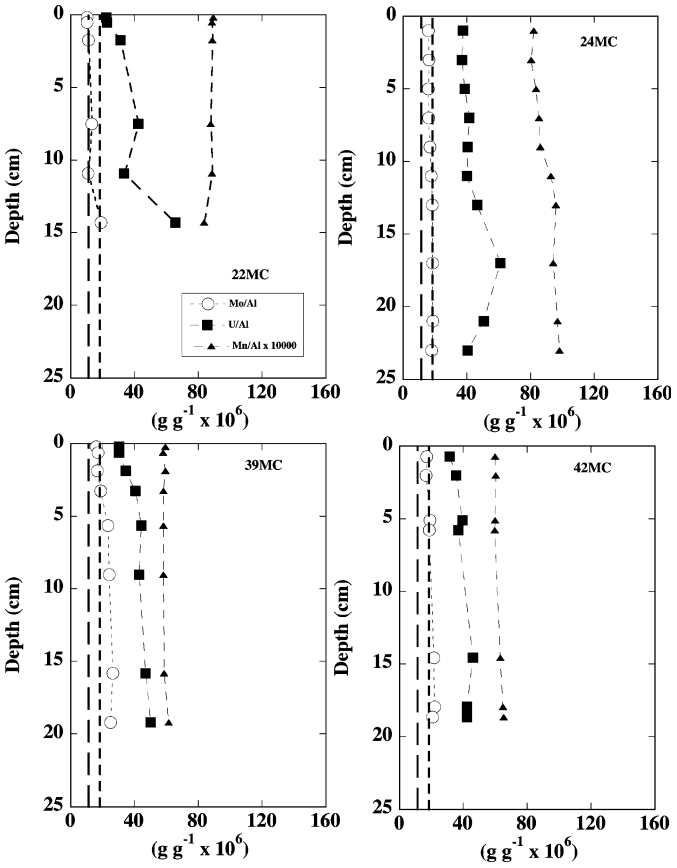

Fig. 5. Solid-phase distributions of Mo/Al, U/Al, and Mn/Al along the Chile margin. Units for Mo and U to Al ratios are as noted along the axis whereas for Mn it is g g^{-1} multiplied by the value listed in the legend of the first panel. The dashed lines represent the Mo:Al and U:Al ratios used as background correction, as discussed in the text. The Chile margin cores, like the Central California margin cores have among the lowest authigenic enrichments.

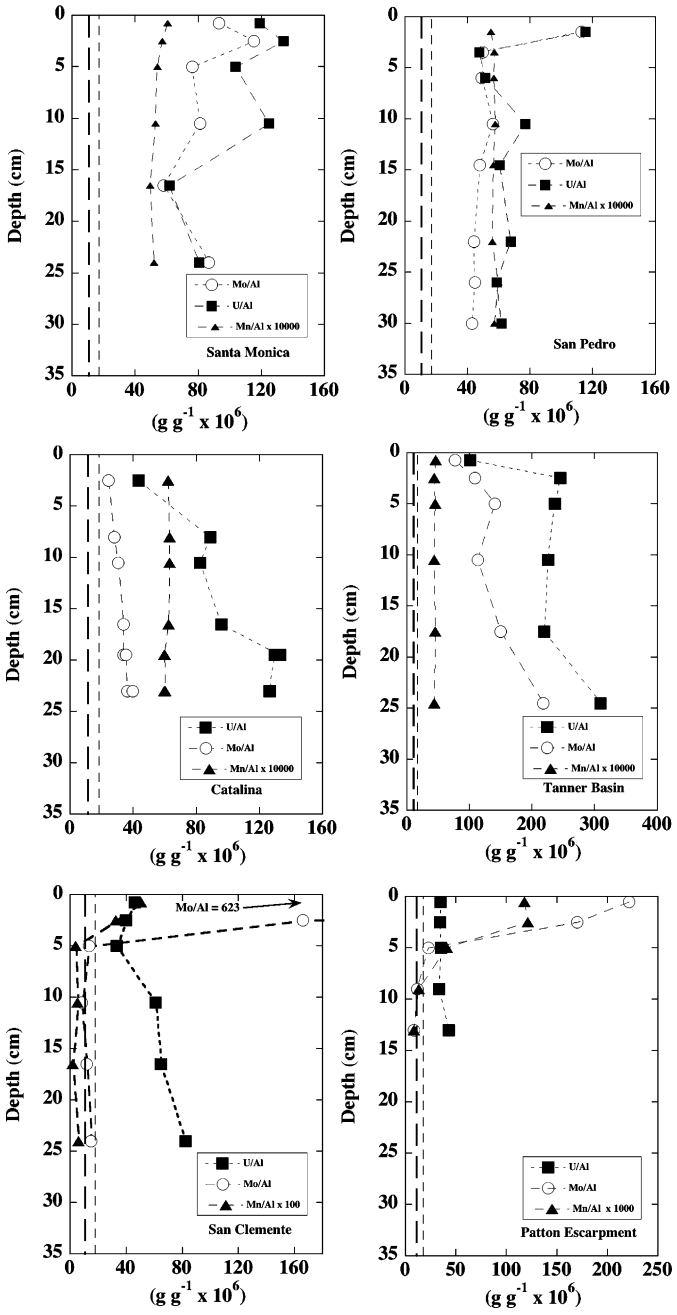

Fig. 6. Solid-phase distributions of Mo/Al, U/Al, and Mn/Al, in the southern California Basin region. Units for Mo and U to Al ratios are as noted along the axis whereas for Mn it is g g^{-1} multiplied by the value listed in the legend. The dashed lines represent the Mo:Al and U:Al ratios used as background correction. Both the San Clemente basin and the Patton Escarpment sites have high near-surface Mn and Mo enrichments, presumably because Mo is adsorbed to Mn-oxide surfaces. Note the changing scales as identified in the figure legends.

for U (>~1 mmol C_{org} m^{-2} day^{-1}, Fig. 8C). The combined data set suggests a Mo:C_{org} rain ratio of $\sim 16 \pm 3$ (2σ) nmol Mo $mmol^{-1}$ C_{org}. Because the rain rate is the sum of the organic carbon burial and oxidation rates, unaccounted for uncertainties in the calculation of the organic carbon oxidation rate, and temporal variability add to uncertainties in the relationship presented, we are thus reticent to apply too much significance to this particular value.

The Mo:C_{org} burial ratio is $\sim 17 \pm 3$ (2 σ) nmol Mo $mmol^{-1}$ C_{org}. This ratio is higher than the Mo:C_{org} from sediment trap material (e.g., 9 ± 3, Nameroff, 1996). The higher value in the sediments is nevertheless consistent because we would expect a higher sediment ratio if more of the organic carbon is remobilized within the sediments than Mo (i.e., diagenesis should increase the ratio), or if additional Mo is added during diagenesis. Data from anoxic basins indicate a greater Mo accumulation rate as a function of organic carbon rain (range 30–230 nmol Mo $mmol^{-1}$ C_{org}; Table 4). This range is consistent with an average anoxic basin burial ratio of ~100 nmol Mo $mmol^{-1}$ C_{org}, which we calculate from the data presented in Algeo and Lyons (2006). In restricted anoxic basins that contain dissolved sulfide in the bottom water (e.g., the Black Sea), low dissolved Mo concentrations can limit the amount of Mo sequestered in the sediments, thus making a unique "anoxic" Mo:C_{org} ratio problematic (Algeo and Lyons, 2006); however, on balance the data set suggest

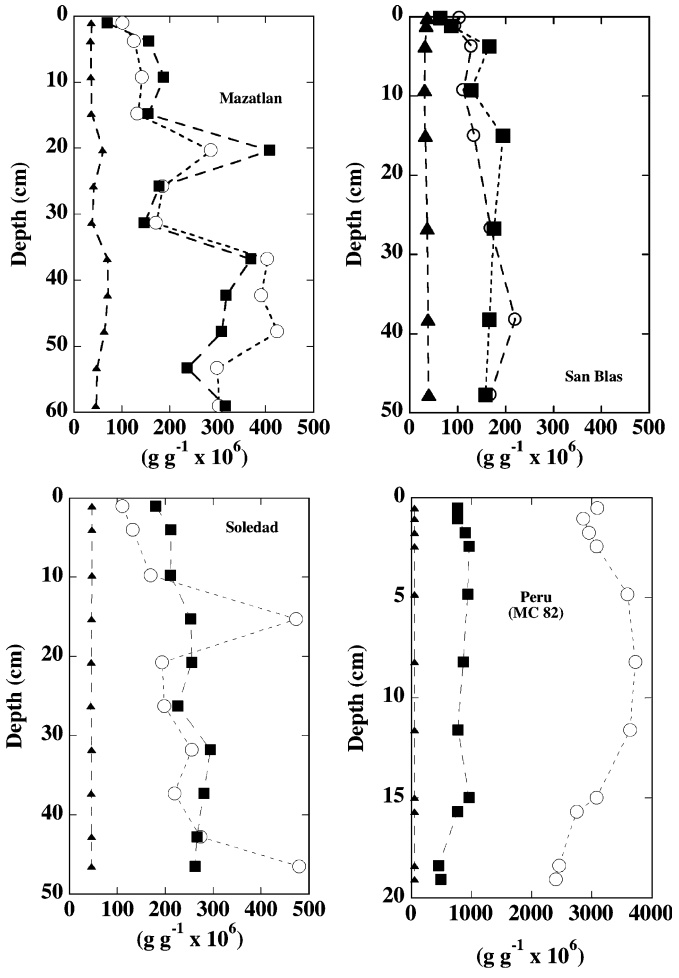

Fig. 7. Solid-phase distributions of Mo/Al, U/Al, and Mn/Al along the Mexico and Peru margins. As a group these sites are the most enriched of the study sites. Units for Mo and U to Al ratios are as noted along the axis whereas for Mn it is g g^{-1} multiplied by the value listed in the legend of the first panel. Because the enrichments are large we do not show the Mo:Al and U:Al ratios used as background correction.

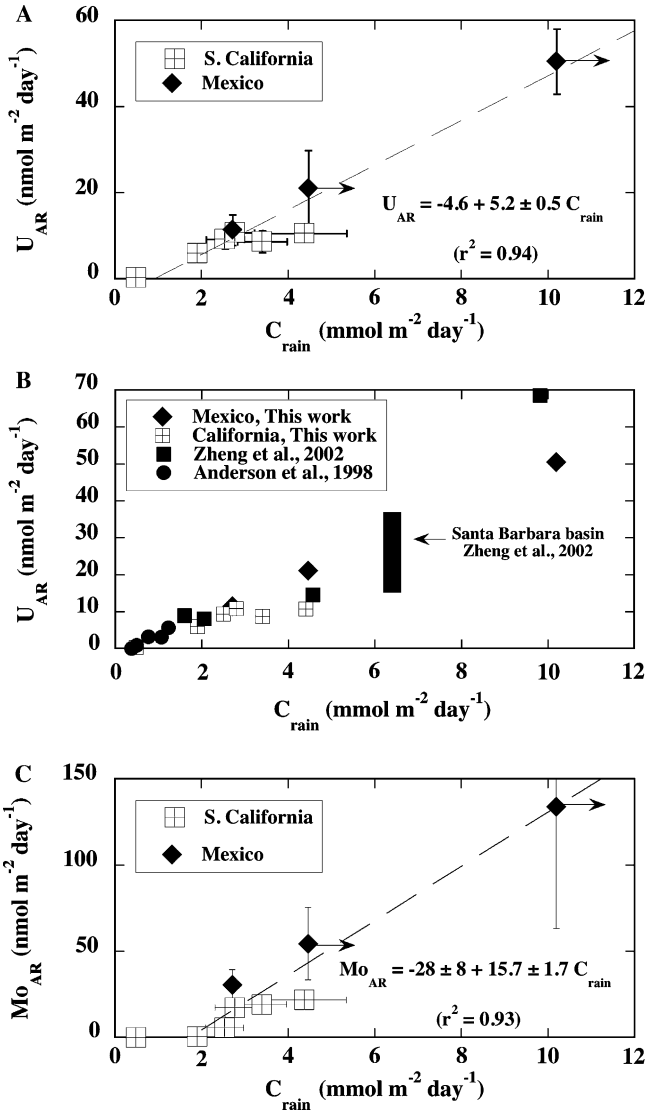

Fig. 8. Uranium (A and B) and molybdenum (C) accumulation rate (U_{AR} and Mo_{AR}) plotted as a function of the organic carbon rain rate. For the sites from this work only (A and C) the organic carbon rain rate is a calculated parameter based on the sum of the organic carbon oxidation rate (C_{ox}) and the organic carbon burial rate (C_{burial}) and is presented in Table 1. The uncertainties are those based on the 1 σ variation in the mean of the concentration or, in the specific case of carbon, the error is the sum of the uncertainties in the carbon oxidation rate and the variation in the average organic carbon concentration. These uncertainties do not include any uncertainties in the accumulation rate as this number appears in both the x and y axis terms, thus these uncertainties cancel. For two of the Mexico margin sites the organic carbon oxidation rate is a minimum value (Poulson et al., 2006), thus we show an arrow indicating the direction of that uncertainty. In the case of prior work (B) the organic carbon rain rate is measured using particle-intercepting sediment traps (Table 4). In the specific case of the Santa Barbara basin (B), Zheng et al. (2002) present a transect of sediment cores through the basin, but only a single sediment trap C_{rain} value.

that the Mo:C_{org} ratio could be more than five times larger in anoxic basins as compared to the open ocean.

One anomaly in our continental margin data set is the Mo:C_{org} ratio of the Peru margin site. This particular site has a ratio that lies between the average anoxic burial ratio and the other continental margin sites (~60–70 nmol Mo $mmol^{-1}$ C_{org}). We speculate that the differences between the Mo:C_{org} ratios, which are most apparent between the anoxic basin and the open-ocean continental margin sites, are driven by changes in the chemical mechanism responsible for Mo authigenesis. This speculation is based on previous work suggesting that there are two "thresholds" for Mo authigeneis, one under low dissolved sulfide conditions and another under high dissolved sulfide conditions (Zheng et al., 2000). As discussed above, under mildly reducing environments authigenesis is dominated by the conversion of the soluble MoO_4^{2-} species to a particle reactive species (e.g., $MoO_xS_{4-x}^{2-}$). This conversion could happen in association with suspended marine particles or within the sediments. As free sulfide concentrations increase, as in anoxic basins, MoO_4^{2-} may be converted directly to MoS_4^{2-} leading to the more efficient removal of dissolved Mo (e.g., Helz et al., 1996 and Section 2.1). It is possible that direct formation of MoS_4^{2-} (under

Table 4
Carbon budget parameters and metal accumulation rates

Site	C_{ox}[a](mmol m^{-2})	C_{burial}[b](day^{-1})	C_{rain}[c]	MAR[d](mg cm^{-2} y^{-1})	Mo[e](nmol m^{-2} day^{-1})	U (nmol m^{-2} day^{-1})
This Study						
Santa Monica	1.9 ± 0.2 (3)	1.5 ± 0.4 (1.8)	3.4 ± 0.6 (3.7)	16	19 ± 3	9 ± 3
San Pedro	1.8 ± 0.4 (1)	2.6 ± 0.6 (2.6)	4.4 ± 1.0 (4.4)	29	22 ± 2	11 ± 2
Catalina	1.3 ± 0.1 (2)	1.2 ± 0.3 (1.4)	2.5 ± 0.4 (2.7)	14	6 ± 1	9 ± 2
Tanner	1.0 ± 0.3 (3)	1.8 ± 0.2 (1.4)	2.8 ± 0.5 (2.4)	12	17 ± 6	11 ± 2
San Clemente	1.0 ± 0.1 (2)	(0.9)	(1.9)	15	0.6 ± 0.6	6 ± 1
Patton Escarp.	0.4 ± 0.1 (2)	(0.08)	(0.5)	3	~0	0.4 ± 0
Mazatlan	1.1	1.7 ± 0.1	2.8	9	30 ± 9	11 ± 4
San Blas	>1.3	3.2 ± 0.2	4.5	21	54 ± 21	21 ± 9
Soledad	>1.8	8.4 ± 0.3	10.2	50	134 ± 71	51 ± 8
Peru		8.3 ± 0.8		(25)	545 ± 56	54 ± 10
Anderson et al. (1998)						
San Clemente			1.2			5.3
N. Calif. Margin			0.4			0.0
N. Calif. Margin			1.1			3.1
Equatorial Pacific			0.9			0.5
Western Arabian Sea			0.8			3.2
Zheng et al. (2000,2002)						
Santa Barbara Basin			6.4		15–350	17.3–34.5
Framvaren			4.6		337	14.5
Black Sea			2.1		69	8.1
Cariaco Basin			1.6		206	9.0
Saanich Inlet			9.8		2226	68.5
Sundby et al. (2004)						
Laurentian Trough					7.1–123	4.7–20.8
Nammeroff (1996)						
Mexico Margin					0.5–208	1–27

[a] C_{ox} is the organic carbon oxidation rate. Estimates for the California margin are averages from multiple sources (in parentheses) (McManus et al., 1997; Berelson et al., 1996; Hammond et al., 2004). Values for the Mexico margin are from Berelson et al. (2005) and Poulson et al. (2006). For San Blass and Soledad these are minimum values because of curvature in the pore fluid CO2 distributions.

[b] C_{burial} is the organic carbon burial rate, which is a product of the percent organic carbon and the mass accumulation rate. Values in parentheses are those reported in Berelson et al. (1996).

[c] C_{rain} is the organic carbon rain rate, which is calculated as $C_{ox} + C_{burial}$ for this study and the uncertainties are the added uncertainties. Values in parentheses are those reported in Berelson et al. (1996).

[d] MAR is the sediment mass accumulation rate and values are taken from Berelson et al. (1996) and Poulson et al. (2006).

[e] Mo_{AR} and U_{AR} are the authigenic Mo and U accumulation rates, which are calculated from the average authigenic concentration reported in Table 4 and the reported MAR. The values reported in McManus et al. (2005) are recalculated here and are slightly smaller than those values because of a spreadsheet error in the calculation of the lithogenic correction.

sulfide-rich conditions) will result in higher Mo accumulation rates per unit of organic carbon flux than for conditions where thiomolybdate species are dominant. One possible interpretation of the Peru margin site is that there is a mix of Mo enrichment mechanisms that drive metal authigenesis at this particular location leading to a Mo:C_{org} ratio that is intermediate between the two Mo enrichment mechanisms. This idea is consistent with the Peru margin being a location where the sediments are highly sulfidic (e.g., Böning et al., 2004), and it was hypothesized by these authors that the near-surface presence of H_2S leads to the observed enhanced Mo enrichments.

There is a possibility that relationships between authigenic metal accumulation and organic carbon delivery to the seabed (Fig. 8) are artifacts of a close coupling between the factors that control organic carbon preservation and the preservation of authigenic metals. Some of these factors could include bottom water oxygen content, sediment mixing, and sediment lithology (e.g., Hedges and Keil, 1995). Indeed, if there is a commonality in preservation, we would expect a close coupling between metal and organic carbon burial, which we observe (Fig. 9). In the specific case of Mo, and as implied above, an alternative master variable is sulfur preservation. This assertion is logical if indeed Mo chemistry is closely coupled to the sulfur cycle as proposed by multiple authors (references as above). If sulfur preservation were important for Mo preservation any relationship between organic carbon burial and Mo accumulation (Fig. 9B) could be primarily a function of the close coupling between organic carbon and sulfur burial and authigenic Mo accumulation and sulfur burial. As an extension of this idea, one place where the fraction of total carbon preserved is low (i.e., low carbon burial efficiencies), yet where carbon flux is high is in mobile sediment or "fluidized sediment beds" found in some deltaic regions (Hedges and Keil, 1995; Aller, 1998). These deposits undergo

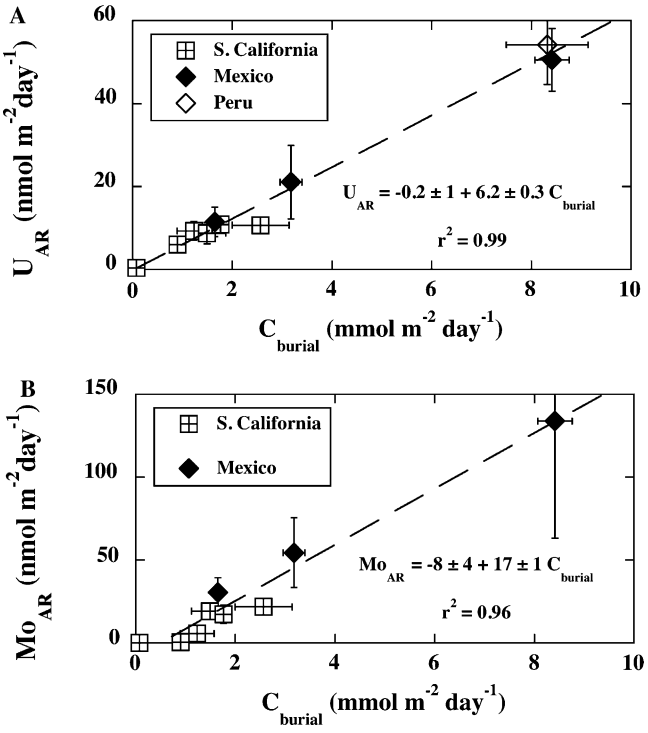

Fig. 9. Uranium (A) and molybdenum (B) accumulation rate (U_{AR} and Mo_{AR}) plotted as a function of the organic carbon burial rate for the sites presented in this work. The close coupling between these parameters suggests that the factors that influence organic carbon burial may also influence authigenic metal burial. Uncertainties are assigned based on the 1 σ variation in the average constituent concentration.

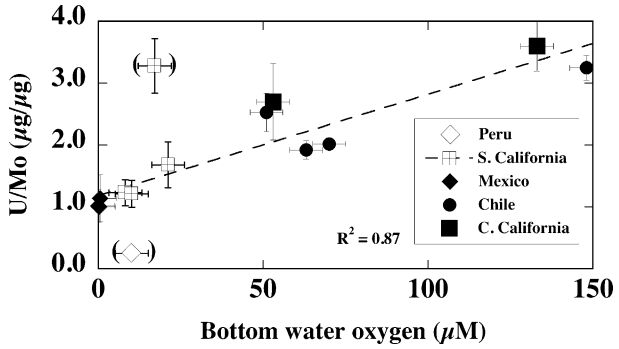

Fig. 10. The U:Mo ratio as a function of bottom water oxygen. Our selection of bottom water oxygen concentrations is as follows: Sta. 02 = 53 μM; Sta. 03 = 133 μM; 22MC = 148 μM; 24MC = 51 μM; 39MC = 63 μM; 42MC = 70 μM; Mazatlan = 0.2 μM; San Blas = 0 μM; Soledad = 0.5 μM; Catalina = 17 μM; San Pedro = 8 μM; Santa Monica = 10 μM; and Tanner Basin = 21 μM. Some of the variability or scatter in the relationship is likely caused by uncertainties in the long-term average bottom water oxygen concentration. As discussed within the text, these values indeed vary and we estimate that variability is likely to be ±5 μM. Uncertainties in the U:Mo ratio are those reported in Table 3 and are based on the 1σ variation in the average value. Values in parentheses are not used in the linear fit.

multiple oxidation and reduction cycles because they are physically disturbed multiple times (Aller, 1998). As a result of this reoxidation process, electron transport can be dominated by species other than sulfate (Aller, 1998), and the multiple reoxidation process leaves behind very little organic carbon for burial. Our prediction from this particular scenario would be that these deposits would also have negligible to small authigenic metal enrichments despite the quite high organic carbon delivery rates, which is consistent with what has been observed (Breckel et al., 2005).

The data presented here point to the potential for quantitative relationships between metal authigenesis and the carbon cycle; however, the exact mechanisms that govern those relationships remain uncertain. Our data also suggest that the U:Mo ratio is at least somewhat sensitive to bottom water oxygen concentration (Fig. 10). This relationship may arise because on one hand both elements are sensitive to organic carbon burial (e.g., Fig. 9), but they have a slightly different sensitivity to some chemical parameter related to bottom water oxygen concentration. One possibility is the presence of dissolved sulfide in pore fluids; however, we do not have the data to verify that idea, but suggest it here as a working hypothesis. Furthermore, there are likely to be a number of environments where this relationship (Fig. 10) will not hold. For example our Sta. 09 has no significant authigenic Mo (Table 3), thus the relationship is not applicable. Also, sites having Mn-rich sediments are unlikely to be applicable because of Mo adsorption onto Mn-oxide phases (San Clemente and Patton Escarpment fall into this category). The Catalina Basin site (diamond in parentheses) has a particularly high ratio and we have no explanation for this data point. Post-depositional sediment transport, a common occurrence on continental margins, might tend to draw the U:Mo ratio to anomalously higher values because of re-exposure of sediment to oxygen. This process will likely affect both U and Mo (e.g., Crusius and Thomson, 2003; Crusius et al., 2004), but could influence Mo more because of its sensitivity to reduced sulfur preservation. Thus, sites where sediment is not subjected to physical disturbances are more likely to provide valuable quantitative insights regarding proxy development than are sites where these disturbances are common.

6.3. Mo burial rates and budgetary implications

From the combination of our own data, along with previously reported data (Table 4), it appears that continental margin sediments could be an important sink for Mo. However, most of our data indicating Mo accumulation are from restricted basins or the open margins along Mexico and Peru, which likely represent end-members in terms of their organic carbon and Mo burial. In combination, the data must be considered limited at this point, but it is noteworthy that the continental margin accumulation rates reported in the literature and offered here range from 0 to >500 nmol m^{-2} day^{-1} (Table 4).

The two suggested Mo inputs to the global ocean are (1) rivers at 1.8×10^8 mol y^{-1} (Martin and Meybeck, 1979 as reviewed in Morford and Emerson, 1999) and (2) low temperature hydrothermal weathering at 0.2×10^8 mol y^{-1} (McManus et al., 2002; Wheat et al., 2002). The primary

sink fluxes are believed to be (1) oxic sediments, with an estimated rate of 0.9×10^8 mol y^{-1}; (2) anoxic sediments at $0.2–0.8 \times 10^8$ mol y^{-1}; and (3) high temperature hydrothermal removal ($<0.2 \times 10^8$ mol y^{-1}) (values reviewed in Morford and Emerson, 1999). These numbers imply a near geochemical balance if the anoxic basin value is about equal to the oxic sink. However, based on our current understanding of the Mo isotope budget, this is not a reasonable assumption (e.g., Siebert et al., 2003). This work considers these two sinks as the primary sinks for Mo and demonstrates that the oxic to anoxic sink ratio must be approximately 0.7 oxic sink to 0.3 anoxic (Siebert et al., 2003). This particular study has a number of uncertainties that the authors identify. However, we could further constrain the Mo anoxic flux based on the amount of carbon currently being sequestered in anoxic basins (1×10^{12} g C_{org} y^{-1}; Hedges and Keil, 1995) and the ratio of buried Mo to organic carbon in these basins (~100 nmol Mo $mmol^{-1}$ C_{org}; Table 4 and Algeo and Lyons, 2006). We should note that this ratio is likely to be an upper limit because the Black Sea ratio is low, yet this particular basin is large. From this approach the amount of Mo being buried in anoxic basins is estimated to be 0.08×10^8 mol y^{-1}. Taking this estimate and the oxic sink at face value implies that there is a deficit of nearly half the Mo input to the oceans, ~1x10^8 mol Mo y^{-1}. This would have to be considered an upper limit for the Mo accumulation in margin sediments.

If we reconsider the paired Mo and isotope budget (i.e., Siebert et al., 2003; Anbar et al., 2004) with the assumption that some Mo must be sequestered in continental margin sediments and the isotope composition of that Mo is 1.6‰ (Poulson et al., 2006), we can construct a revised global budget. Here, we use the conventions proposed previously (Siebert et al., 2003; Anbar et al., 2004) with two additions; an isotope value for the continental margin sink as well as values for the low temperature hydrothermal source of Mo:

$$\delta_L F_L + \delta_H F_H = \delta_O F_O + \delta_M F_M + \delta_A F_A$$

where, δ and F are the isotope values and flux for each component (references as above unless otherwise noted) and, L represents the lithogenic source($F_L = 1.8 \times 10^8$ mol y^{-1}, $\delta = 0$‰, e.g., Anbar et al., 2004), H the low temperature hydrothermal source ($F_H = 0.2 \times 10^8$ mol y^{-1}, δ;= 0.8‰, McManus et al., 2002), O the oxic sink ($F_O = 0.9 \times 10^8$ mol y^{-1}, $\delta = -0.8$‰, Anbar et al., 2004; Poulson et al., 2006), M the margin sink ($F_M = X$, mol y^{-1}, $\delta = 1.6$‰, Poulson et al., 2006), and A the anoxic sink ($F_H = 0.1 \times 10^8$ mol y^{-1}, $\delta = 2.0$‰). The isotope value for the lithogenic (weathering) source is tentative, but it is based on previously published data (after Siebert et al., 2003), the oxic, continental margin, and anoxic basin isotope values are reviewed in Poulson et al., 2006. Because there is a limited amount of isotope data to describe each of the sources and sinks, this balance approach must be viewed cautiously (e.g., Anbar et al., 2004). However, to achieve an isotope balance, the continental margin flux needs to be $\sim 0.4 \times 10^8$ mol Mo y^{-1}. This value leaves a significant imbalance in the flux budget, requiring an additional sink term of $\sim 0.6 \times 10^8$ mol Mo y^{-1}, and highlights the uncertainty in our understanding of the global Mo budget. Furthermore, a final note of caution to this budgetary approach arises because of the long residence time of Mo (~0.8 milion years) relative to the likely glacial–interglacial variations in the ocean carbon and associated trace metal fluxes—particularly along continental margins (e.g., ~10–100 ky). There is insufficent information at this point to fully evaluate the impact of short term variations on the Mo isotope balance; however, it is reasonable to assume that there could be some impact.

Although we could tie the Mo burial rate directly to the burial of organic carbon based on the Mo to C_{org} burial ratio (Fig. 9B) and the more well-characterized organic carbon burial budget (Hedges and Keil, 1995), the fact that there is a positive intercept along the x-axis precludes this approach directly. However, we can consider the predicted margin flux of 0.4×10^8 mol Mo y^{-1} within the context of the organic carbon burial budget simply to assess if such burial is reasonable. There are approximately 6×10^{15} mmol C_{org} buried per year in non-deltaic shelf and slope environments (Hedges and Keil, 1995), if there was Mo buried with all of this carbon with a Mo:C_{org} burial ratio of 17 ± 3 nmol $mmol^{-1}$ (Fig. 9B), $\sim 0.8 \pm 0.2 \times 10^8$ mol Mo y^{-1} would be buried in these settings. However, as noted above, not all of the continental margin sediments accumulate sufficient organic carbon to also accumulate Mo (i.e., Fig. 9 has a positive intercept), thus this particular estimate is too high. If, however, half of the sediments accumulating organic carbon along the continental margin accumulate at a rate sufficient to accumulate Mo then there is agreement between the two estimates.

One final way to consider the Mo budget is in terms of the extent of reducing environments within the ocean. It is likely that significant Mo authigenesis requires environments sufficiently reducing that oxygen penetrates into the sediments less than 1 cm depth (e.g., Morford and Emerson, 1999). Archer et al. (2002) calculate that ~20% of the seafloor is sufficiently reducing that oxygen penetration is <1 cm; however, based on the data presented here it is unlikely that 20% of the seafloor would actually be accumulating significant Mo. If, however, only 1% of the seafloor (3.6 km^2, Menard and Smith, 1966) maintains the conditions conducive for most of the 0.4 mol Mo y^{-1} burial, then the accumulation rate of Mo would have to be 30 nmol m^{-2} day^{-1}. This value for the Mo accumulation rate is at least 10 times smaller than that for the Peru Margin and is smaller than many estimates for the Mexico margin, Santa Barbara basin, and the Laurentian Trough (Table 4). However, it is larger than a number of the other continental margin estimates proposed here. Although we suspect that more than 1% of the seafloor actually accumulates Mo and it is likely that 30 nmol m^{-2} day^{-1} is not an accurate mean accumulation rate, this calculation in light of our other calculations and the previously published data demonstrates a set of reasonable assumptions that support our contention that continental margins are an important Mo sink.

7. Conclusions

Data presented here suggest that authigenic U and Mo are tightly coupled to either organic carbon delivery to the seafloor or to the organic carbon burial rate. In the particular case of Mo this coupling may be related to a mutual relationship between these two variables and sulfur burial. Despite their common sensitivity to organic carbon cycling, in combination these elements also exhibit some sensitivity to the concentration of bottom water oxygen. Further work is required to refine our understanding of how these elements are influenced by the global biogeochemical cycles of carbon and oxygen.

Based on the burial budget of organic carbon and on the Mo:C_{org} burial ratio and the Mo isotope and flux budgets we estimate that continental margin environments accumulate authigenic Mo at a rate of 0.4×10^8 mol y^{-1}. Based on the Mo:C_{org} burial ratio and the carbon budget for anoxic basins, these environments sequester $\sim 0.1 \times 10^8$ mol Mo y^{-1} of the total Mo. If previous estimates for Mo input to the oceans are accurate ($\sim 2 \times 10^8$ mol Mo y^{-1}) then our estimates for the Mo sinks in combination with those from the literature are insufficient to achieve a geochemical balance, and to achieve both an isotope and flux balance, both the oxic and continental margin sinks would need to be revised upward.

Appendix A Comparison of sediment digestion techniques

Reference[a]	Sample ID[b]	Al (%)	±	Fe (%)	±	Ti (μg/g)	±	Mn (μg/g)	±
BCR-1	F7-A, B, C	6.98	0.02	9.70	0.16	13147	166	1475	12
	S7-A, B, C	7.36	0.11	9.68	0.13	13770	125	1467	8
	M7-A, B, C	7.29	0.14	9.67	0.07	13538	91	1468	9
	Average	**7.21**	**0.20**	**9.68**	**0.01**	**13485**	**315**	**1470**	**4**
	Reference	**7.22**		**9.39**		**13428**		**1394**	
AGV-1	F5-A, B, C	8.77	0.14	4.58	0.06	5881	116	716	15
	S5-A, B, C	9.12	0.05	4.72	0.07	6227	67	703	18
	M5-A, C	8.99	0.05	4.86	0.20	6395	322	776	20
	Average	**8.96**	**0.18**	**4.72**	**0.14**	**6168**	**262**	**732**	**39**
	Reference	**9.07**		**4.73**		**6355**		**744**	
W-2	F6-A, B, C	8.14	0.19	7.79	0.11	6356	46	1343	24
	S6-A, B, C	8.43	0.04	7.81	0.13	6525	45	1333	4
	M6-A, B, C	8.43	0.30	7.84	0.22	6537	254	1341	29
	Average	**8.34**	**0.17**	**7.81**	**0.03**	**6473**	**101**	**1339**	**5**
	Reference	**8.12**		**7.51**		**6355**		**1262**	
MAG-1	F4-A, B, C	8.22	0.07	4.71	0.08	3952	28	727	12
	S4-A, B, C	8.50	0.10	4.76	0.04	4085	56	701	2
	M4-A, B, C	5.10	0.65	4.80	0.10	4167	56	736	20
	Average	**7.27**	**1.88**	**4.75**	**0.04**	**4068**	**109**	**721**	**18**
	Reference	**8.66**		**4.76**		**4502**		**759**	
SX12279	F2-A, B, C	0.46	0.01	0.25	0.01	111	8	1498	44
	S2-A, B, C	0.36	0.01	0.22	0.01	81	9	1656	28
	M2-A, B, C	0.41	0.01	0.25	0.01	113	5	1647	35
	Average	**0.41**	**0.05**	**0.24**	**0.02**	**102**	**18**	**1600**	**89**
	Reference	**0.43**		**0.29**		**125**		**1693**	
SX12280	F3-A, B, C	5.58	0.07	3.58	0.04	2913	29	2306	28
	S3-A, B, C	5.63	0.05	3.49	0.02	2871	22	2320	8
	M3-A, B, C	6.11	0.06	3.84	0.05	3153	55	2570	17
	Average	**5.77**	**0.29**	**3.63**	**0.18**	**2979**	**152**	**2399**	**149**
	Reference	**5.95**		**4.01**		**3243**		**2570**	
NS1750M	F1-A, B, C	3.55	0.05	2.30	0.02	1848	7	256	3
	S1-A, B, C	3.82	0.05	2.45	0.04	1999	10	256	7
	M1-A, B, C	3.91	0.07	2.52	0.01	2092	23	274	4
	Average	**3.76**	**0.19**	**2.42**	**0.11**	**1980**	**123**	**262**	**10**
	Reference	**3.80**		**2.47**		**2109**		**286**	

Bold font indicates average and ± values.

[a] Reference materials are either from the U.S.G.S. (BCR-1, AGV-1, W-2, and MAG-1) or are in-house reference materials (SX12279, SX12280, and NS1750M) as described in the text.

[b] Sample IDs designate the method of digestion where samples with an F are those done by fusion, S indicates hot plate assisted digestions, and M indicates microwave assisted digestions.

Acknowledgment

Many individuals have provided invaluable assistance during the cruises when these data were collected, those individuals are too numerous to mention here, but their contributions are no less important to the success of our work. The captains and crews of the R.V. Pt. Sur, R.V. New Horizon, and R.V. Roger Revelle are all extended sincere gratitude for their tireless efforts collecting the sediments, and we note our use of the Pt. Sur on multiple occasions. A number of senior colleagues also participated in collecting the samples used during this study and were gracious with their time and effort at sea and we acknowledge them: Kenneth Johnson, Kenneth Coale, Alan Mix, Nick Pisias, and David Burdige. Bobbi Conard, Andy Ross, and Andy Ungerer provided invaluable analytical support for many of the measurements made in the laboratory. Finally, it is impossible to acknowledge all in the scientific community who have had an impact on the development of the ideas presented here, however incomplete those ideas may yet be. We therefore acknowledge the thoughtful discussions and criticisms of the many who have been willing to ask the provocative question or offer guidance. Their unselfish cooperation is appreciated. Associate Editor Tim Shaw, Jennifer Morford, Lex van Geen, Hans Brumsack, and six anonymous reviewers provided constructive criticism on early versions of this manuscript. This research was supported by NSF Grants OCE-0219651 and OCE-9911550 to the lead P.I. and OCE-9617929 to J.M. and G.P.K.; NSF Grants OCE-0002250 and OCE-0129555 to W.M.B.

Associate editor: Timothy J. Shaw

References

Algeo, T.J., Lyons, T.W., 2006. Mo-TOC covariation in modern anoxic marine environments: Implications for analysis of paleoredox and hydrographic conditions. *Paleoceanography* **21**, PA1016. doi:10.1029/2004PA001112, 2006.

Aller, R.C., 1998. Mobile deltaic and continental shelf muds as fluidized bed reactors. *Mar. Chem.* **61**, 143–155.

Anbar, A.D., 2004. Molybdenum stable isotopes: observations, interpretations and directions. In: Johnson, C.M. et al. (Eds.), *Geochemistry of Non-Traditional Stable Isotopes*, Vol. 55. Mineralogical Society of America and Geochemical Society, Washington, pp. 429–454.

Anderson, R.F., 1982. Concentration, vertical flux, and remineralization of particulate uranium in seawater. *Geochim. Cosmochim. Acta* **46**, 1293–1299.

Anderson, R.F., 1987. Redox behaviour of uranium in an anoxic marine basin. *Uranium* **3**, 145–164.

Anderson, R.F., Fleisher, M.Q., Lehuray, A.P., 1989a. Concentration, oxidation-state, and particulate flux of uranium in the Black-Sea. *Geochim. Cosmochim. Acta* **53**, 2215–2224.

Anderson, R.F., Fleisher, M.Q., Lehuray, A.P., Murray, J.W., 1989b. Uranium deposition in Saanich Inlet sediments, Vancouver Island. *Geochim. Cosmochim. Acta* **53**, 2205–2213.

Anderson, R.F., Kumar, N., Mortlock, R.A., Froelich, P.N., Kubik, P., Dittrich-Hannen, B., Sutter, M., 1998. Late-Quaternary changes in productivity of the Southern Ocean. *J. Mar. Syst.* **17**, 497–514.

Archer, D.E., Morford, J.L., Emerson, S.E., 2002. A model of suboxic sedimentary diagenesis suitable for automatic tuning and gridded global domains. *Global Biogeochem. Cycles* **16**, 1017. doi:10.1029/2000GB00128.

Barnes, C.E., Cochran, J.K., 1990. Uranium removal in oceanic sediments and the oceanic U balance. *Earth Planet. Sci. Lett.* **97**, 94–101.

Barnes, C.E., Cochran, J.K., 1993. Uranium geochemistry in estuarine sediments: controls on removal and release processes. *Geochim. Cosmochim. Acta* **57**, 555–569.

Barnett, P.R.O., Watson, J., Connelly, D., 1984. A multiple corer for taking virtually undisturbed samples from shelf, bathyal, and abyssal sediments. *Oceanol. Acta* **7**, 399–408.

Berelson, W.M., 1991. The flushing of two deep sea basins, Southern California borderland. *Limnol. Oceanog.* **36**, 1150–1166.

Berelson, W.M., Hammond, D.E., 1986. The calibration of a new free-vehicle benthic flux chamber for use in the deep-sea. *Deep-Sea Res.* **33**, 1439–1454.

Berelson, W.M., Hammond, D.E., Johnson, K.S., 1987. Benthic fluxes and cycling of biogenic silica and carbon in two southern California borderland basins. *Geochim. Cosmochim. Acta* **51**, 1345–1363.

Berelson, W.M., McManus, J., Coale, K.H., Johnson, K.S., Kilgore, T., Burdige, D.J., Pilskaln, C., 1996. Biogenic matter diagenesis on the sea floor: a comparison between two continental margin transects. *J. Mar. Res.* **54**, 731–762.

Berelson, W.M., Prokopenko, M., Sansone, F.J., Graham, A., McManus, J., Bernhard, J.M., 2005. Anaerobic diagenesis of silica and carbon in continental margin sediments: discrete zones of TCO_2 Production. *Geochim. Cosmochim. Acta* **69**, 4611–4629.

Berrang, P.G., Grill, E.V., 1974. The effect of manganese oxide scavenging on molybdenum in Saanich Inlet, British Columbia. *Mar. Chem.* **2**, 125–148.

Bertine, K.K., 1972. The deposition of molybdenum in anoxic waters. *Mar. Chem.* **1**, 43–53.

Bertine, K.K., Turekian, K.K., 1973. Molybdenum in marine deposits. *Geochim. Cosmochim. Acta* **48**, 605–615.

Bloch, S., 1980. Some factors controlling the concentration of uranium in the world ocean. *Geochim. Cosmochim. Acta* **44**, 373–377.

Böning, P., Brumsack, H-J., Böttcher, M.E., Schnetger, B., Kriete, C., Kallmeyer, J., Borchers, S.L., 2004. Geochemistry of Peruvian near-surface sediments. *Geochim. Cosmochim. Acta* **21**, 4429–4451.

Bostick, B.C., Fendorf, S., Helz, G.R., 2003. Differential adsorption of molybdated and tetrathiomolybdate on pyrite (FeS_2). *Environ. Sci. Technol.* **37**, 285–291.

Breckel, E.J., Emerson, S., Balistrieri, L.S., 2005. Authigenesis of trace metals in energetic tropical shelf environments. *Cont. Shelf Res.* **25**, 1321–1337.

Brewer, P.G., 1975. Minor elements in seawater. In: Riley, J.P. (Ed.), *Chemical Oceanography*, Vol. 1. Academic Press, pp. 415–496.

Brumsack, H.-J. (1986). The inorganic geochemistry of cretaceous black shales (DSDP Leg 41) in comparison to modern upwelling sediments from the Gulf of California. In: Summerhayes, C.P., Shackleton, N.J. (Eds.), *North Atlantic Paleoceanography*, Geological Society of America Special Paper 21, Boulder, Colorado, pp. 447–462.

Brumsack, H.-J., Gieskes, J., 1983. Interstitial water trace-metal chemistry of laminated sediments form the Gulf of California, Mexico. *Mar. Chem.* **14**, 89–106.

Calvert, S.E., Pedersen, T.F., 1993. Geochemistry of recent oxic and anoxic marine sediments: Implications for the geological record. *Mar. Geol.* **113**, 67–88.

Carpenter, J.H., 1965. The Chesapeake Bay Institute technique for the Winkler dissolved oxygen method. *Limnol. Oceanogr.* **10**, 141–143.

Chaillou, G., Anschutz, P., Lavaux, G., Schäfer, J., Blanc, G., 2002. The distribution of Mo, U, and Cd in relation to major redox species in muddy sediments of the Bay of Biscay. *Mar. Chem.* **80**, 41–59.

Chase, Z., Anderson, R.F., Fleisher, M.Q., 2001. Evidence from authigenic uranium for increased productivity of the glacial Subantarctic Ocean. *Paleoceanography* **16**, 1–11.

Chen, J.H., Wasserburg, G.J., Damm, K.L.V., Edmond, J.M., 1986. The U–Th–Pb systematics in hot springs on the East Pacific Rise at 21°N and the Guaymas Basin. *Geochim. Cosmochim. Acta* **50**, 2467–2479.

Church, T.M., Sarin, M.M., Fleisher, M.Q., Ferdelman, T.G., 1996. Salt marshes: an important coastal sink for dissolved uranium. *Geochim. Cosmochim. Acta* **60**, 3879–3887.

Cochran, J.K., 1982. The oceanic chemistry of the U- an Th-series nuclides. In: Ivanovich, M., Harmon, R.S. (Eds.), *Uranium Series Disequilibrium: Applications to Environmental Problems*. Clarendon, Oxford, pp. 384–430.

Cochran, J.K., Carey, A.E., Sholkovitz, E.R., Suprenant, L.D., 1986. The geochemistry of uranium and thorium in coastal marine sediments and sediment porewaters. *Geochim. Cosmochim. Acta* **50**, 663–680.

Cole, J.J., Lane, J., Marino, R., Howarth, R.W., 1993. Molybdenum assimilation by cyanobacteria and phytoplankton in freshwater and salt water. *Limnol. Oceanogr.* **38**, 25–35.

Collier, R.W., 1985. Molybdenum in the Northeast Pacific Ocean. *Limnol. Oceanogr.* **30**, 1351–1354.

Colodner, D.C., Edmond, J.M., Boyle, E.A., 1995. Rhenium in the Black Sea: comparison with molybdenum and uranium. *Earth Planet. Sci. Lett.* **131**, 1–15.

Crusius, J., Calvert, S., Pedersen, T., Sage, D., 1996. Rhenium and molybdenum enrichments in sediments as indicators of oxic, suboxic and sulfidic conditions of deposition. *Earth Planet. Sci. Lett.* **145**, 65–78.

Crusius, J., Pedersen, T.F., Kienast, S., Keigwin, L., Labeyrie, L., 2004. Influence of northwest Pacific productivity on North Pacific Intermediate Water oxygen concentrations during the Bølling–Ållerød interval (14.7–12.9 ka). *Geology* **32**, 633–636.

Crusius, J., Thomson, J., 2003. Mobility of authigenic rhenium, silver, and selenium during postdepositional oxidation in marine sediments. *Geochim. Cosmochim. Acta* **67**, 265–273.

Degens, E.T., Khoo, K., Michaelsis, W., 1977. Uranium anomaly in Black Sea sediments. *Nature* **269**, 566–569.

Dorta, C.C., Rona, E., 1971. Geochemistry of uranium in the Cariaco Trench. *Bull. Mar. Sci* **21**, 754–765.

Dunk, R.M., Mills, R.A., Jenkins, W.J., 2002. A reevaluation of the oceanic uranium budget for the Holocene. *Chem. Geol.* **190**, 45–67.

Emerson, S.R., Huested, S.S., 1991. Ocean anoxia and the concentrations of molybdenum and vanadium in seawater. *Mar. Chem.* **34**, 177–196.

Emery, K.O., 1960. *The Sea Off Southern California*. John Wiley and Sons, New York, 366 p..

Erickson, B.E., Helz, G.R., 2000. Molybdenum (VI) speciation in sulfidic waters: stability and lability of thiomolybdates. *Geochim. Cosmochim. Acta* **64**, 1149–1158.

Fredrickson, J.K., Zachara, J.M., Kennedy, D.W., Duff, M.C., Gorby, Y.A., Li, S.W., Krupka, K.M., 2000. Reduction of U(VI) in goethite (α-FeOOH) suspensions by a dissimilarory metal-reducing bacterium. *Geochim. Cosmochim. Acta* **64**, 3085–3098.

Ganeshram, R.S., Calvert, S.E., Pedersen, T.F., Cowie, G.L., 1999. Factors controlling the burial of organic carbon in laminated and bioturbated sediments off NW Mexico: implications for hydrocarbon preservation. *Geochim. Cosmochim. Acta* **63**, 1723–1734.

Gilmore, G., Hemingway, J.D., 1995. *Practical Gamma-Ray Spectrometry*. Wiley, New York, 314 pp.

Hammond, D.E., Cummins, K.M., McManus, J., Berelson, W.M., Smith, G., Spagnoli, F., 2004. A comparison of methods for benthic flux measurement along the California margin: shipboard core incubations vs. in situ benthic landers. *Limnol. Oceanogr. Methods* **2**, 146–159.

Hartnett, H.E., Devol, A.H., 2003. Role of strong oxygen-deficient zone in the preservation and degradation of organic matter: a carbon budget for the continental margins of the northwest Mexico and Washington State. *Geochim. Cosmochim. Acta* **67**, 247–264.

Hedges, J.I., Keil, R.G., 1995. Sedimentary organic matter preservation: an assessment and speculative synthesis. *Mar. Chem.* **49**, 81–115.

Hedges, J.I., Stern, H., 1984. Carbon and nitrogen determinations of carbonate-containing solids. *Limnol. Oceanogr.* **29**, 657–663.

Helz, G.R., Miller, C.V., Charnock, J.M., Mosselmans, J.F.W., Pattrick, R.A.D., Garner, C.D., Vaughan, D.J., 1996. Mechanism of molybdenum removal from the sea and its concentration in black shales: EXAFS evidence. *Geochim. Cosmochim. Acta* **60**, 3631–3642.

Howarth, R.W., Cole, J.J., 1985. Molybdenum availability, nitrogen limitation and phytoplankton growth in natural waters. *Science* **229**, 653–655.

Howarth, R.W., Marino, R., Cole, J.J., 1988a. Nitrogen fixation in freshwater, estuarine and marine ecosystems. 2. Biogeochemical controls. *Limnol. Oceanogr.* **33**, 688–701.

Howarth, R.W., Marino, R., Lane, J., Cole, D.R., 1988b. Nitrogen fixation in freshwater, estuarine and marine ecosystems. 1. Rates and importance. *Limnol. Oceanogr.* **33**, 669–687.

Ingall, E.D., Jahnke, R.A., 1994. Evidence for enhanced phosphorous regeneration from marine sediments overlain by oxygen-depleted waters. *Geochim. Cosmochim. Acta* **58**, 2571–2575.

Jahnke, R.A., Reimers, C.E., Craven, D.B., 1990. Intensification of recycling of organic matter at the sea floor near ocean margins. *Nature* **348**, 50–54.

King, S.L., Froelich, P.N., Jahnke, R.A., 2000. Early diagenesis of germanium in sediments of the Antarctic South Atlantic: in search of the missing Ge sink. *Geochim. Cosmochim. Acta* **64**, 1375–1390.

Knauss, K., Ku, T.-L., 1983. The elemental composition and decay-series radio-nuclide content of plankton from the east Pacific. *Chem. Geol.* **39**, 125–145.

Ku, T.-L., Knauss, K., Mathieu, G.G., 1977. Uranium in the open ocean: concentration and isotopic composition. *Deep-Sea Res.* **24**, 1005–1017.

Kumar, N., Anderson, R.F., Mortlock, R.A., Froelich, P.N., Kubib, P., Dittrich-Hannen, B., Suter, M., 1995. Increased biological productivity and export production in the glacial Southern Ocean. *Nature* **378**, 675–680.

Legeleux, F., Reyss, J.L., Bonte, P., Organo, C., 1994. Concomitant enrichments of uranium, moybdenum and arsenic in suboxic continental-margin sediments. *Oceanol. Acta* **17**, 417–429.

Lovley, D.R., Phillips, E.J.P., Gorby, Y.A., Landa, E.R., 1991. Microbial reduction of uranium. *Nature* **350**, 413–416.

Lovley, D.R., Roden, E.E., Phillips, E.J.P., Woodward, J.C., 1993. Enzymatic iron and uranium reduction by sulfate-reducing bacteria. *Mar. Geol.* **113**, 41–53.

Lyons, T.W., Werne, J.P., Hollander, D.J., Murray, R.W., 2003. Contrasting sulfur geochemistry and Fe/Al and Mo/Al ratios across the last oxic-to-anoxic transition in the Cariaco Basin, Venezuela. *Chem. Geol.* **195**, 131–157.

Marino, R., Howarth, R.W., Shamess, J., Prepas, E., 1990. Molybdenum and sulfate as controls on the abundance of nitrogen-fixing cyanobacteria in saline lakes in Alberta. *Limnol. Oceanogr.* **35**, 245–259.

Martin, J.M., Meybeck, M., 1979. Elemental mass-balance of material carried by major world rivers. *Mar. Chem.* **7**, 173–206.

McKee, B.A., DeMaster, D.J., Nittrouer, C.A., 1987. Uranium geochemistry on the Amazon shelf: evidence for uranium release from bottom sediments. *Geochim. Cosmochim. Acta* **51**, 2779–2786.

McManus, J., Berelson, W.M., Coale, K.H., Johnson, K.S., Kilgore, T., 1997. Phosphorous regeneration in continental margin sediments. *Geochim. Cosmochim. Acta* **61**, 2891–2907.

McManus, J., Berelson, W.M., Klinkhammer, G.P., Hammond, D.E., Holm, C., 2005. Authigenic uranium: relationship to oxygen penetration depth and organic carbon rain. *Geochim. Cosmochim. Acta* **69**, 95–108.

McManus, J., Hammond, D.E., Cummins, K.M., Klinkhammer, G.P., Berelson, W.M., 2003. Diagenetic Ge–Si fractionation in continental margin environments: further evidence for a non-opal Ge sink. *Geochim. Cosmochim. Acta* **67**, 4545–4557.

McManus, J., Nägler, T.F., Siebert, C., Wheat, C.G., Hammond, D.E., 2002. Oceanic molybdenum isotope fractionation: diagenesis and hydrothermal ridge-flank alteration. *Geochem. Geophys. Geosyst.* **3**, 1078. doi:10.1029/2002GC00035.

Menard, H.W., Smith, S.M., 1966. Hypsometry of ocean basin provinces. *J. Geophys. Res.* **71**, 4305–4324.

Mo, T., Suttle, A.D., Sackett, W.M., 1973. Uranium concentrations in marine sediments. *Geochim. Cosmochim. Acta* **37**, 35–51.

Morford, J.L. (1999). The geochemistry of redox-sensitive trace elements. PhD thesis, University of Washington, p.

Morford, J.L., Emerson, S.R., 1999. The geochemistry of redox sensitive trace metals in sediments. *Geochim. Cosmochim. Acta* **63**, 1735–1750.

Morris, A.W., 1975. Dissolved molybdenum and vanadium in the northeast Atlantic Ocean. *Deep-Sea Res.* **22**, 49–54.

Muller-Karger, F.E., Varela, R., Thunell, R., Luerssen, R., Hu, C., Walsh, J.J., 2005. The importance of continental margins in the global carbon cycle. *Geophys. Res. Lett.* **32**, L01602. doi:10.1029/2004GL02134.

Murray, R.W., Miller, D.J., Kryck, K.A. (2000). Analysis of major and trace elements in rocks, sediments, and interstitial waters by inductively coupled plasma-atomic emission spectrometry (ICP-AES). ODP Tech. Note, 29.

Nameroff, T. (1996) The geochemistry of redox-sensitive metals in sediments of the oxygen minimum off Mexico. PhD thesis, University of Washington, p.

Nameroff, T., Balistrieri, L.S., Murray, J.W., 2002. Suboxic trace metal geochemistry in the eastern tropical North Pacific. *Geochim. Cosmochim. Acta* **66**, 1139–1158.

Palmer, M.R., Edmond, J.M., 1989. The strontium budget of the modern ocean. *Earth Planet. Sci. Lett.* **92**, 11–26.

Paulsen, D.M., Paerl, H.W., Bishop, P.E., 1991. Evidence that molybdenum dependent nitrogen fixation is not limited by high concentrations of sulfate in marine environments. *Limnol. Oceanogr.* **36**, 1325–1334.

Piper, D.Z., Isaacs, C.M., 1995. Minor elements in Quaternary sediment from the Sea of Japan: a record of surface-water productivity and intermediate-water redox conditions. *GSA Bull.* **107**, 54–67.

Potts, P.J., Tindle, A.G., Webb, P.C., 1992. *Geochemical Reference Material Compositions*. CRC Press, London, 313 pp..

Poulson, R.L., Siebert, C., McManus, J., Bereleson, W.M., 2006. Authigenic molybdenum isotope signatures in marine sediments. *Geology* **34** (8), 617–620.

Reimers, C.E., Jahnke, R.A., McCorkle, D.J., 1992. Carbon fluxes and burial rates over the continental slope and rise off central California with implications for the global carbon cycle. *Global Biogeochem. Cycles* **6**, 199–224.

Reimers, C.E., Lange, C.B., Tabak, M., Bernhard, J.M., 1990. Seasonal spillover and varve formation in the Santa Barbara Basin. *Limnol. Oceanog.* **35**, 1577–1585.

Reimers, C.E., Ruttenberg, K.C., Canfield, D.E., Christiansen, M.B., Martin, J.B., 1996. Porewater pH and authigenic phases formed in the uppermost sediments of the Santa Barbara Basin. *Geochim. Cosmochim. Acta* **60**, 4037–4057.

Reimers, C.E., Suess, E., 1983. Spatial and temporal patterns of organic matter accumulation on the Peru continental margin. In: Thiede, J., Suess, E. (Eds.), *Coastal Upwelling its Sediment Record. Part B. Sedimentary Records of Ancient Coastal Upwelling*. Plenum Press, pp. 311–346.

Rosenthal, Y., Boyle, E.A., Labeyrie, L., Oppo, D., 1995. Glacial enrichments of authigenic Cd and U in Sub-Antartic sediments-a climatic control on the elements oceanic budget. *Paleoceanography* **10**, 395–413.

Sani, R.K., Peyton, B.M., Amonette, J.E., Geesey, G.G., 2004. Reduction of uranium(VI) under sulfate-reducing conditions in the presence of Fe(III)-(hydr)oxides. *Geochim. Cosmochim. Acta* **68**, 2639–2648.

Sarin, M.M., Krishnaswami, S., Samayajulu, B.L.K., Moore, W.S., 1990. Chemistry of uranium, thorium, and radium isotopes in the Ganga–Brahmaputra river system-weathering processes and fluxes to the Bay of Bengal. *Geoderma* **54**, 1387–1396.

Scholkovitz, E.R., Gieskes, J.M., 1971. A physical–chemical study of the flushing of the Santa Barbara Basin. *Limnol. Oceanog.* **16**, 479–489.

Shaw, T.J., Gieskes, J., Jahnke, R.A., 1990. Early diagenesis in differing depositional environments: the response of transition metals in pore water. *Geochim. Cosmochim. Acta* **54**, 1233–1246.

Shimmield, G.B., Price, N.B., 1986. The behavior of molybdenum and manganese during early sediment diagenesis-Offshore Baja California, Mexico. *Mar. Chem.* **19**, 261–280.

Siebert, C., Nägler, T.F., Kramers, J.D., 2001. Determination of molybdenum isotope fractionation by double-spike multicollector inductively coupled plasma mass spectrometry. *Geochem. Geophys. Geosyst.* **2**, 2000GC000124.

Siebert, C., McManus, J., Bice, A., Poulson, R.L., Berelson, W.M., 2006. Molybdenum isotope signatures in continental margin marine sedimetns. *Earth Planet. Sci. Let.* **241**, 723–733.

Siebert, C., Nägler, T.F., von Blanckenburg, F., Kramers, J.D., 2003. Molybdenum isotope records as a potential new proxy for paleoceanography. *Earth Planet. Sci. Lett.* **211**, 159–171.

Silverberg, N., Martinez, A., Aguiniga, S., Carriquiry, J.D., Romero, N., Shumilin, E., Cota, S., 2004. Contrasts in sedimentation flux below the southern California current in late 1996 and during the El Nino event of 1997–1998. *Estuarine Coastal Shelf Sci.* **59**, 575–587.

Sundby, B., Martinez, P., Gobeil, C., 2004. Comparative geochemistry of cadmium, rhenium, uranium, and molybdenum in continental margin sediments. *Geochim. Cosmochim. Acta* **68**, 2485–2493.

Tossell, J.A., 2005. Calculating the partitioning of the isotopes of Mo between oxidic and sulfidic species in aqueous solution. *Geochim. Cosmochim. Acta* **69**, 2981–2993.

Tribovillard, N., Riboulleau, A., Lyons, T.W., Baudin, F., 2004. Enhanced trapping of molybdenum by sulfurized organic matter of marine origin in Mesozoic limestones and shales. *Chem. Geol.* **213**, 385–401.

Tuit, C., Waterbury, J., Ravizza, G., 2004. Diel variation of molybdenum and iron in marine diazotrophic cyanobacteria. *Limnol. Oceanogr.* **49**, 978–990.

Turekian, K.K., Wedepohl, K.H., 1961. Distribution of the elements in some major units of the Earth's crust. *GSA Bull.* **72**, 175–192.

Van Geen, A., Zheng, Y., Berhard, J.M., Cannariato, K.G., Carriquiry, J., Dean, W.E., Eakins, B.W., Ortiz, J.D., Pike, J., 2003. On the preservation of laminated sediments along the western margin of North America. *Paleoceanography* **18**, 1098.

Veeh, H.H., Calvert, S.E., Price, N.B., 1974. Accumulation of uranium in sediments and phosphorites on the southwest African Shelf. *Mar. Chem.* **23**, 189–202.

Verardo, D.J., Froelich, P.N., McIntyre, A., 1990. Determination of organic carbon and nitrogen in marine sediments using the Carlo Erba NA-1500. *Deep-Sea Res.* **37**, 157–165.

Vorlicek, T.P., Helz, G.R., 2002. Catalysis by mineral surfaces: implications for Mo geochemistry in anoxic environments. *Geochim. Cosmochim. Acta* **66**, 3679–3692.

Vorlicek, T.P., Kahn, M.D., Kasuya, Y., Helz, G.R., 2004. Capture of molybdenum in pyrite-forming sediments: role of ligand-induced reduction by polysulfides. *Geochim. Cosmochim. Acta* **68**, 547–556.

Wieser, M.E., DeLaeter, J.R., 2000. Molybdenum concentrations measured in eleven USGS Geochemical reference materials by isotope dilution thermal ionisation mass spectrometry. *Geostandard Newsl.* **24**, 275–279.

Wheat, C.G., Mottl, M.J., Rudnicki, M., 2002. Trace element and REE composition of a low-temperature ridge-flank hydrothermal spring. *Geochim. Cosmochim. Acta* **66**, 3693–3705.

Wheatcroft, R.A., Sommerfield, C.K., 2005. River sediment flux and shelf sediment accumulation rates on the Pacific Northwest margin. *Cont. Shelf Res.* **25**, 311–332.

Wilde, P., Lyons, T.W., Quinby-Hunt, M.S., 2004. Organic carbon proxies in black shales: molybdenum. *Chem. Geol.* **206**, 167–176.

Yamada, M., Tsunogai, S., 1983/84. Postdepositional enrichment of uranium in sediment from the Bering Sea. *Mar. Geol.* **54**, 263–276.

Zheng, Y., Anderson, R.F., van Geen, A., Fleisher, M.Q., 2002. Preservation of particulate non-lithogenic uranium in marine sediments. *Geochim. Cosmochim. Acta* **66**, 3085–3092.

Zheng, Y., Anderson, R.F., van Geen, A., Kuwabara, J., 2000. Authigenic molybdenum formation in marine sediments: a link to pore water sulfide in the Santa Barbara Basin. *Geochim. Cosmochim. Acta* **64**, 4165–4178.